3 Symmetric Thin Liquid Films with Fluid Interfaces

Dimo Platikanov and Dotchi Exerowa

CONTENTS

3.1 Introduction 128
3.2 Experimental Methods for Research of Emulsion Films 130
3.2.1 The Problem: "Film Thickness" 130
3.2.2 Microscopic Emulsion or Foam Films 132
3.2.3 Black WOW Emulsion Films 134
3.2.4 Measurement of the Disjoining Pressure 136
3.2.5 Measurement of the Contact Angles 137
3.3 Thinning and Rupture of Thin Liquid Films; Black Spot Formation 138
3.3.1 Kinetics of Thinning of Plane-Parallel Liquid Films 139
3.3.2 Deviations from the Plane-Parallel Film During its Thinning 142
3.3.3 Rupture of Thin Liquid Films 145
3.3.4 Jump-Like Formation of Black Spots in an Emulsion or Foam Film 147
3.4 Thermodynamics of Thin Emulsion and Foam Films 149
3.4.1 The Simplified Film Model 150
3.4.2 Mechanical Equilibrium of a Thin Emulsion or Foam Film 150
3.4.3 Fundamental Thermodynamic Equations of a Thin Liquid Film 153
3.4.4 Thermodynamic Approach with Two Gibbs Dividing Planes 154
3.4.5 Contact Between a Thin Emulsion or Foam Film and the Adjacent Bulk Liquid 158
3.5 Surface Forces in Thin Emulsion and Foam Films 159
3.5.1 DLVO Surface Forces: Theoretical 160
3.5.1.1 Electrostatic Disjoining Pressure 160
3.5.1.2 van der Waals Disjoining Pressure 161
3.5.2 DLVO Surface Forces: Experimental 162
3.5.2.1 Experiments with Foam Films 162
3.5.2.2 Experiments with Emulsion Films 164
3.5.2.3 Potential of the Diffuse Double Layer at the Film's Interface 165
3.5.3 Steric Surface Forces 166
3.5.4 Oscillatory Disjoining Pressure 169
3.6 Black Emulsion and Foam Films 170
3.6.1 Two Equilibrium Phase States of Black Films 170
3.6.2 Disjoining Pressure in Black Films 171
3.6.2.1 Ionic Surfactants 172
3.6.2.2 Nonionic Surfactants 173
3.6.2.3 Phospholipids 173
3.6.3 Properties of CBF and NBF and the Transition between Them 175
3.6.4 Stability and Rupture of Bilayer Black Films 177
3.7 Similarity between Emulsion Films and Foam Films 181
References 182

3.1 INTRODUCTION

Thin liquid films arise spontaneously in all colloid and disperse systems with a liquid disperse media. They are formed always when two particles of the disperse phase (solid particles, liquid drops, or gas bubbles) come close to each other. The liquid film is a symmetric film when both approaching particles originate from the same disperse phase with the same composition of substances, i.e., the symmetric liquid film divides two equal micro-phases. Such thin liquid films are the emulsion films, the foam films, and the films between the particles of a sol. In more complicated cases, when two particles with different composition of substances approach each other, an asymmetric liquid film is formed. These are all cases of heterocoagulation. The most important asymmetric films are the wetting films – thin liquid films which divide a solid and a gas phase.

The *emulsion films* are symmetric liquid films between two liquid phases, i.e., L′LL′ films, L′ being a liquid immiscible with the liquid L. One can distinguish two types of emulsion films: *OWO films* and *WOW films*, which correspond to the two emulsion types. Accordingly the *foam films* are GLG films. Both emulsion and foam films are thin liquid films with fluid interfaces. Only these types of films are considered in the present chapter. Since the foam films are more extensively studied, most of the examples which illustrate different aspects of the thin liquid films with fluid interfaces are foam films. The similarity between emulsion and foam films allows information obtained about foam films to be used for emulsion films and vice versa. This similarity is specially discussed in Section 3.7.

Obviously the properties and the behavior of the thin liquid films determine the stability or instability of the corresponding disperse system. That is why the thin liquid film is one of the most important objects of the colloid and interface science. Furthermore the liquid films play a central role in many technological processes. All this caused the vast expansion of the fundamental and applied research of thin liquid films, especially in the second half of the twentieth century. However, the first observation on the properties and behavior of thin liquid films were reported in the eighteenth century.

The prominent scientists Hook and Newton described the process of thinning of foam films and the formation of black spots and black films in a thicker film [1]. This is the reason that the current IUPAC nomenclature refer to the thinnest emulsion or foam films as "Newton black films." In the middle of the nineteenth century the Belgian scientist Plateau performed extensive investigations of the properties of the thin liquid films [2]. He established the important fact that the thin liquid film is always connected either with a bulk liquid phase or with a solid wall through a liquid body with concave surfaces. We call now this liquid body "Plateau border." Marangoni studied [3] the role of the expansion or compression of the surfactant adsorption layers for the stability of the films, known now as the "Marangoni effect." The great Gibbs gave significant ideas concerning the liquid film's stability [4], among them the so-called "Gibbs elasticity."

During the twentieth century, studies on thin liquid films expanded at accelerated rates. In the first decades Perrin studied extensively the different types of black foam films as well as the interesting phenomenon of stratification [5]. In 1936 Derjaguin introduced [6] the quantity *disjoining pressure* – the most important thermodynamic parameter which characterizes the thin liquid film. The great success of the DLVO theory for the stability of the lyophobic colloids [7,8] put forward the decisive role of the thin liquid films for the stability of all types of disperse systems with liquid disperse media. Significant contributions for the quantitative description of thin liquid films have been carried out by the scientific schools of Derjaguin (Russia), Overbeek (Netherlands), Mysels (U.S.A.), Scheludko (Bulgaria), and many others.

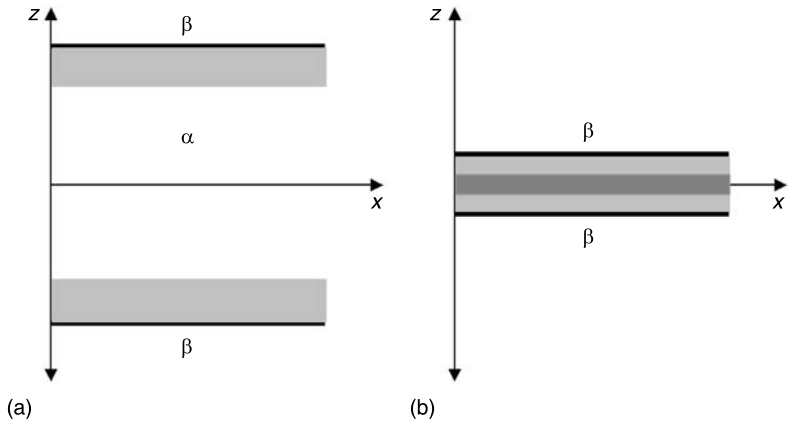

FIGURE 3.1 (a) Scheme of a "thick" liquid film and (b) scheme of a thin liquid film formed from the liquid phase α between two equal fluid phases β.

What exactly should we call a *thin liquid film*? Let us consider a symmetric liquid film with parallel plane interfaces (Figure 3.1). The Cartesian coordinate system is oriented so that the x and y axes lie in the film plane, while the z-axis is normal to the film interfaces. Obviously, the film dimension along z is much smaller than the dimensions along x and y which determine the film area. However, the question arises: what is much smaller?

The liquid phase from which the film is formed is denoted in Figure 3.1 by α and the adjacent phase (another liquid or gas) by β. The α/β interface is actually not a mathematical plane but an interfacial layer with final thickness. Most of the physical quantities inside this interfacial layer vary along the z-axis, due to the mutual influence of the phases α and β. When the distance between both interfaces is rather large (Figure 3.1(a)), the two interfacial layers are far away from each other. There is liquid between them with the same properties as in the bulk liquid phase α. For instance such a L′LL′ system should be considered as a system of three bulk liquid phases, although one of the liquid phases' shape is a film. Such a liquid film is a *thick film* from the viewpoint of the thermodynamics; nevertheless its thickness could be few micrometers only.

In the case when the film thickness is small enough so that both interfacial layers overlap (Figure 3.1(b)), there is no liquid inside the film with the properties of the bulk liquid phase α. Just like in a single interfacial layer most of the physical quantities vary along the z-axis over the entire liquid film from the bulk of the one phase β up to the other phase β. As we shall see later, this is the physical ground for the rise of the disjoining pressure in the film as well as for the change of the surface tension of the film interfaces. Some properties of the film become dependent on its thickness. Such a film is referred to as a thin liquid film.

It should be noted that this is a thermodynamic definition of the thin liquid film and it reflects the peculiar properties of the thin film and their thickness dependence. However, when kinetic properties (e.g., film drainage, rheology, dynamic elasticity, etc.) are considered, often the liquid film is called "thin" simply because of its very small thickness, not taking into account that it could be a thermodynamically "thick" film. For instance, Gibbs has considered the foam film elasticity assuming the same surface tension of the film surfaces as that of the bulk liquid.

The thermodynamic definition of the thin liquid film shows that the most important factor, which determines its properties, is the interaction between the two film interfaces, i.e., the interactions due to different type surface forces between the two adjacent phases across the liquid film. The total Gibbs energy of interaction $G(h)$ depends on the film thickness h. It determines a force per unit film area:

$$\Pi = -[\partial G(h)/\partial h]_{p,T} \tag{3.1}$$

The pressure Π is called the *disjoining pressure*, which is positive in the case of repulsion between the film interfaces, and negative in the case of attraction. Later we shall consider a mechanical definition of the disjoining pressure as well (Section 3.4).

The single thin liquid films of all types are very useful models for investigation of pair interactions (disjoining pressure, interaction energy, stability or instability, etc.). Thus the thin liquid film has attained its own significance as being a powerful tool (both experimental and theoretical) in colloid and interface science. On the other hand, as already noticed, the properties of thin liquid films are decisive for the properties of the corresponding disperse system, e.g., an emulsion. Certainly, the emulsion system is not simply a sum of many liquid films. It is much more complicated. Nevertheless, knowledge of film's properties significantly advances the elucidation of a problem when investigating a real emulsion.

3.2 EXPERIMENTAL METHODS FOR RESEARCH OF EMULSION FILMS

The peculiar properties of thin liquid films cannot be studied using the well known physicochemical methods for investigation of bulk phases and even of single interfaces. Original and unique methods have been developed for liquid film research. The increase of our knowledge about thin liquid films is due, to a great extent, to the effective experimental techniques created for their investigation. This chapter focusses on symmetric thin liquid films with fluid interfaces, i.e., emulsion films and foam films. Accordingly, the experimental methods for mainly emulsion films are considered in this section.

3.2.1 The Problem: "Film Thickness"

Film thickness is the most important quantity to be experimentally determined. It not only characterizes the thin liquid film but also most film properties depend on the thickness. Obviously, the thickness h of a thin liquid film is defined as the distance between the two film interfaces. The quantity h would be exactly defined if the film interfaces were mathematical faces. However, this is not the case for symmetric films with fluid interfaces. The definition of their film thickness is very difficult. The transition from the liquid film to the adjacent liquid (or gas) phase is not abrupt. There is an interfacial layer with finite thickness even in a one-component liquid film. However, the emulsion and foam films contain more components; at least a surfactant which forms adsorption layers at the film interfaces. The complicated structure of the film interfacial layers requires special definition of the mathematical face that could be accepted as a film boundary.

One possibility is the mechanical definition: the film boundaries are two plane-parallel mathematical faces, each of which is subject to a uniform, isotropic tension. These faces are the *surfaces of tension*. The *mechanical film thickness* is defined as the distance h between the two surfaces of tension [9].

The thermodynamic description of an interface is based on the so-called *Gibbs dividing plane*. The thin liquid film thermodynamics involves two Gibbs dividing planes (see Section 3.4).

The position of these planes is defined by a special condition, which can be chosen by us. It is most appropriate for thin liquid films to accept zero interfacial excess of the main component in the liquid film, i.e., of the liquid which is solvent in the bulk phase from which the film is formed. Under this condition the position of both Gibbs dividing planes of the film is defined and the *thermodynamic film thickness* is the distance between these two planes [10,11]. The thermodynamic film thickness should be used when data for the quantities characterizing the film are treated with thermodynamic relations.

The big problem is that neither the mechanical nor the thermodynamic film thickness exactly coincides with the thickness which is experimentally determined using different physical methods. Most of these methods are optical methods and the measurement of the film thickness is based on the abrupt change of properties such as the refractive index and electron density at the film boundary. In the case of electric methods for film thickness measurement, again an abrupt change at the film boundary of specific conductivity, dielectric permitivity, for example, is required. The thin liquid film definition presented in Section 3.1 shows that most of the physical quantities vary along the normal to the film over the entire liquid film and some film properties are thickness dependent. Moreover there is no abrupt transition at the interface film/adjacent phase. That is why the real physical thickness is not directly measured through the experimental methods used.

Let us consider the most widely used optical method – the interferometric method, based on measurement of the intensity of visible light reflected from an emulsion film. Classical optics provides relations that link the thickness of the film with its optical characteristics [12]. If emulsion films are observed in white light, it can be seen that during thinning their coloration changes periodically. Initially, the process runs rather rapidly and gradually slows down. Such a course of the interference can be registered as a curve photocurrent/time in which the extrema correspond to the interference maxima and minima, i.e., film thicknesses are divisible to $\lambda/4n$ (where λ is the wavelength of light and n is the refractive index of the liquid in the film). Thus, knowing the order k of interference, it is easy to determine the film thickness at these points. Film thickness (between a maximum and a minimum) is calculated from the ratio between the intensities measured of the reflected monochromatic light I, corresponding to a certain thickness, and $I_{\max}$, corresponding to the interference maximum, according to the formula [13]

$$h_w = \frac{\lambda}{2\pi n}\left(k\pi \pm \arcsin\sqrt{\frac{I/I_{\max}}{1+\left[4N/(1-N)^2\right](1-I/I_{\max})}}\right) \tag{3.2}$$

with $N = (n-n')^2/(n+n')^2$, n' being the refractive index of the liquid in the adjacent phases; h_w is called equivalent film thickness, i.e., the thickness of an emulsion film with uniform refractive index n of the bulk solution from which the film is formed. For foam films Equation 3.2 transforms [14] into

$$h_w = \frac{\lambda}{2\pi n}\left(k\pi \pm \arcsin\sqrt{\frac{I/I_{\max}}{1+\left[\left(n^2-1\right)/2n\right]^2(1-I/I_{\max})}}\right) \tag{3.3}$$

The accuracy of thickness measurements with the interferometric technique is $\pm$ 0.2 nm.

It is clear that h_w is not equal to the real physical film thickness. Although h_w does not coincide with the thermodynamic thickness h, h_w is close to it, if the last is defined through the condition of zero interfacial excess of the solvent in the film. The difference between h_w and h could be neglected for thicknesses larger than 30 nm. However, for thinner liquid films it is necessary to account also for the film structure. The three-layer film model ("sandwich model")

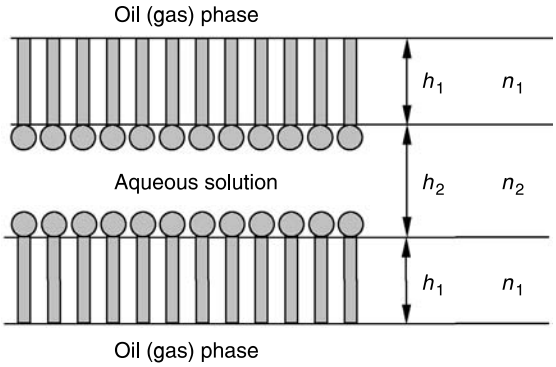

FIGURE 3.2 A three-layer model ("sandwich model") of an OWO emulsion film or a foam film: an aqueous layer with thickness h_2 and refractive index n_2 between two hydrocarbon layers with thickness h_1 and refractive index n_1.

with an aqueous core of thickness h_2 and refractive index n_2 and two homogenous layers of hydrocarbon chains of the adsorbed surfactant of thickness h_1 each and refractive index n_1 is often used for foam films (Figure 3.2). The thickness of the aqueous core h_2 is most often determined, according to the formula [15]

$$h_2 = h_w - 2h_1 \frac{n_1^2 - 1}{n_2^2 - 1} \tag{3.4}$$

The same film model and Equation 3.4 can be adapted to aqueous emulsion films as well.

Since each model involves some assumptions, the calculation of h_2 always renders certain inaccuracy. The most important problem in the three-layer model concerns the position of the plane that divides the hydrophobic and hydrophilic parts of the adsorbed surfactant molecule. In some cases it seems reasonable to have this plane passing through the middle of the hydrophilic head of the molecule, in others the head does not enter into the aqueous core. A more detailed model is the five-layer model in which the aqueous layer (Figure 3.2) is divided into three layers: two layers contain the hydrophilic parts of the adsorbed molecules and the inner core contains aqueous solution only. The calculations of the film thickness based on different film models do not solve the general thickness problem. However, they provide possibilities for reasonable interpretation of the experimental results.

3.2.2 Microscopic Emulsion or Foam Films

Small circular emulsion or foam films, the radius of which is within the range of 10 to 500 μm, are considered to be microscopic films. The experimental technique for their study has been most successful and is constantly being improved. It allows thermodynamic quantities to be measured, kinetic behavior to be followed, the formation of black films to be recorded, and the formation of metastable states to be realized, for example. An advantage is the possibility to work at very low surfactant concentrations.

The measuring cell of Scheludko and Exerowa [16] has proven to be a suitable and reliable tool for the formation of microscopic horizontal emulsion or foam films. It is shown in Figure 3.3,

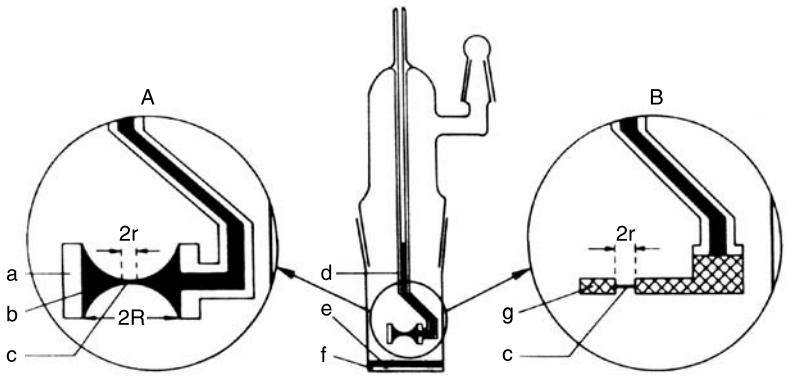

FIGURE 3.3 Scheme of the measuring cell for the study of microscopic emulsion or foam films. A: in a glass tube; B: in a porous plate; **a** is the glass tube film holder; **b** is a biconcave drop; **c** is the microscopic emulsion or foam film; **d** is a glass capillary; **e** is surfactant solution (in case of foam film only); **f** is optically flat glass; **g** is the porous plate; *r* is the film radius; *R* is the film holder radius. (After Refs. 16, 18, and 38.)

variants A and B. The microscopic film c is formed in the middle of a biconcave drop b, situated in a glass tube a of radius *R*, by withdrawing liquid from it (variant A) and in the hole of porous plate g (variant B). Typical photographs of different states of an emulsion microscopic film (non-equilibrium film with dimpling, relatively thick film, black spots, black film) taken under a microscope are presented in Figure 3.4. The suitable tube radius *R* in variant A is 0.2 to 0.6 cm and the film radius ranges from 100 to 500 μm. In variant B the hole radius can be considerably smaller, for instance 120 μm, and, respectively, the film radius can be 10 μm. The film holder with the film is situated in the closed space of the cell, filled with the second liquid (or saturated with the solution vapor in the case of a foam film). The periphery of the film is in contact with the first liquid phase, of the solution from which the film is formed. The film holders, the tube or the porous plate, are welded to capillary d. In the case of aqueous emulsion or foam films, the inner part of the tube a, carrying the biconcave drop, is finely "furrowed" with vertical lines, closely situated to one another, which improve wetting [17]. In the case of "oil" films the film holder should be made hydrophobic. A constant capillary pressure acts on the film formed in part A in Figure 3.3. It is determined by the radius of curvature of the meniscus.

Porous plates of various pore radii can be used in part B [18], Figure 3.3. If the meniscus penetrates into the pores, their radius determines the radius of curvature, i.e., the small pore size allows to increase the capillary pressure until the gas phase can enter in them (in the case of foam films). The capillary pressure can be increased to more than 10^5 Pa, depending on the pore size and the surface tension of the solution.

Another measuring cell for microscopic films has been specially designed [19] for emulsion films (Figure 3.5). Vessel 1 contains the first liquid – the solution from which the emulsion film is formed. The tubes 2 situated co-axially contain the second liquid of the adjacent phases. This liquid forms two menisci at the orifices of both tubes. Using the micrometric pistons 3 the two menisci can be very precisely put close to each other until the microscopic emulsion film is obtained between them. The film is observed and its thickness can be interferometrically measured through the plane-parallel glass window 4 by the microscope 5.

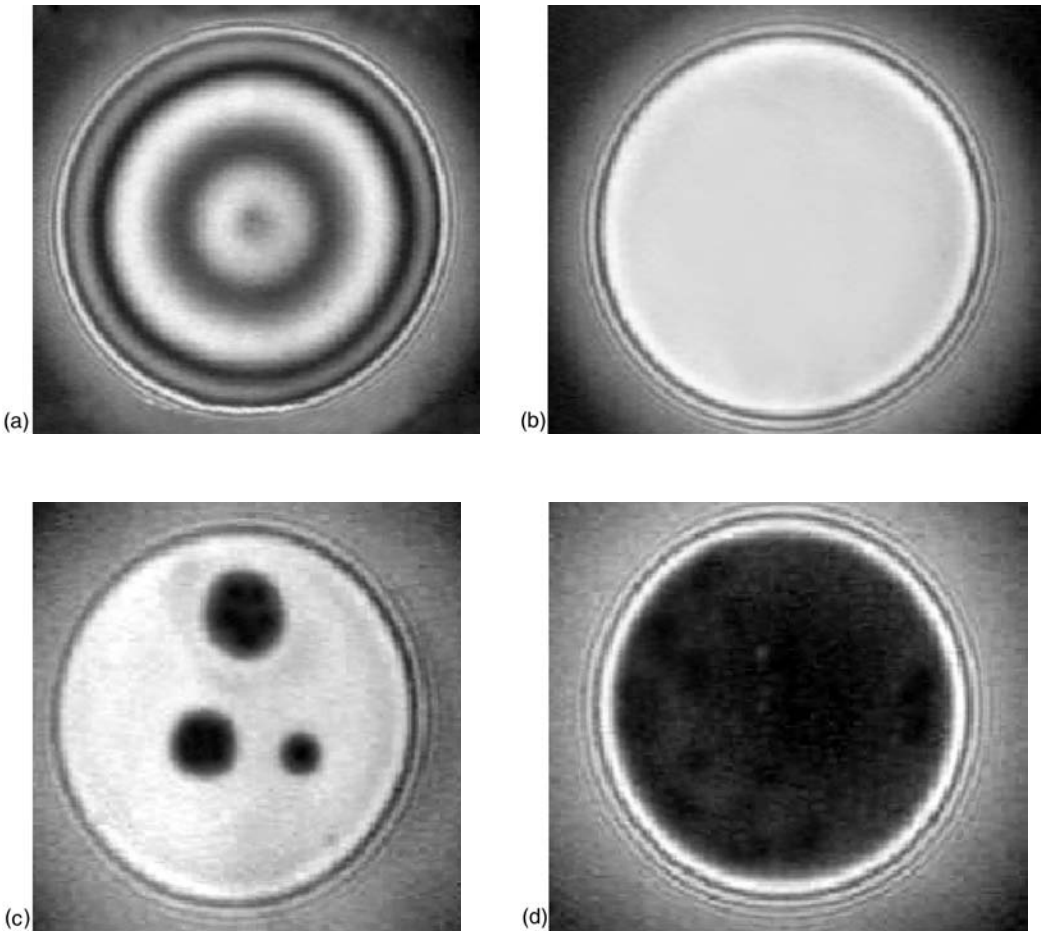

FIGURE 3.4 Typical photographs of a microscopic thin emulsion film taken under a microscope: (a) non-equilibrium film with dimpling; (b) relatively thick equilibrium film; (c) non-equilibrium film with black spots in it; (d) equilibrium black film.

3.2.3 Black WOW Emulsion Films

Black "oil" emulsion films between aqueous phases (often denoted as *bilayer lipid membranes* or BLM) are usually obtained in the cell [20] schematically presented in Figure 3.6. The vessel which contains the aqueous solution 1 is divided in two compartments by the teflon wall 3. There is a small hole with sharp edges in this wall. A drop of the "oil" – a surfactant solution in a nonpolar solvent – is put in the hole using a fine pipette 4. A small vertical emulsion film from this nonpolar liquid is formed in the hole. It drains quickly due to gravity until a *Newton black emulsion film* is formed in the hole. In case the surfactant used is a phospholipid the Newton black emulsion film is called bilayer lipid membrane. It is observed and investigated using the light source 6 and the microscope 7. For research of some electrical properties of such films the two electrodes 5 are used.

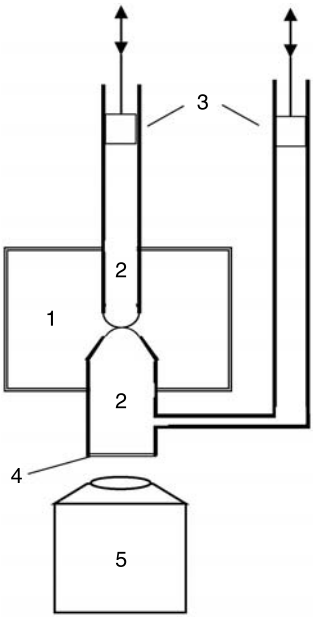

FIGURE 3.5 Principle scheme of a measuring cell for the study of microscopic emulsion films. 1 is a glass vessel with the liquid (phase α) from which the emulsion film is formed; 2 are glass tubes with the other liquid (phase β) of the adjacent phases; 3 are fine micrometric pistons; 4 is a plane-parallel glass plate; 5 is a microscope.

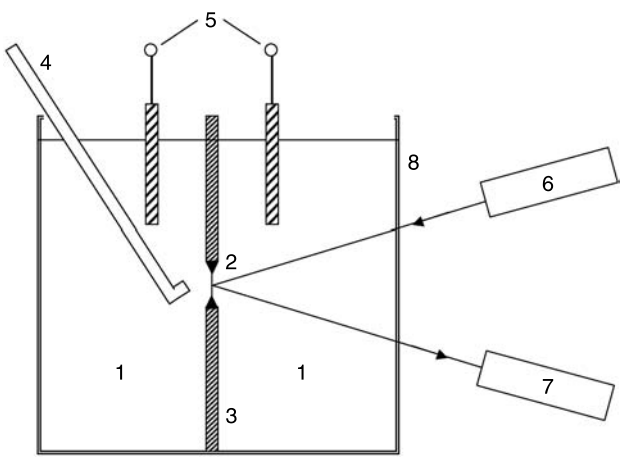

FIGURE 3.6 Principle scheme of a measuring cell for the study of black WOW emulsion films including bilayer lipid membranes (BLM). 1 are two compartments of the vessel 8 which contain aqueous solution – the liquid of the adjacent phases β; 2 is the WOW black emulsion film formed in a small hole in the Teflon wall 3; 4 is a fine pipette filled with the nonpolar liquid solution (phase α); 5 are electrodes; 6 is a light source; 7 is a microscope.

3.2.4 Measurement of the Disjoining Pressure

The disjoining pressure Π due to the surface forces acting in the film is the most important thermodynamic quantity which determines the film stability. The experimental techniques described in subsection 3.2.2 are usually used for determination of Π as well. At equilibrium Π is equal to the pressure difference Δp applied from outside to the film (see Section 3.4). For microscopic horizontal circular emulsion or foam films (Figure 3.3) Δp is the capillary pressure of the concave meniscus around the film, determined by the meniscus curvature and the interfacial tension of the bulk solution. Δp is experimentally accessible and at equilibrium $\Pi = \Delta p$ can be determined. Let us consider this case more closely since it is the base of the successful and widely used experimental method *Thin Liquid Film–Pressure Balance Technique* [21].

A block scheme of the apparatus is shown in Figure 3.7. The films are formed in the porous plate measuring cell (Figure 3.3, part B). The hydrodynamic resistance in the porous plate is sufficiently small and the maximum capillary pressure which can be applied to the film is determined by the pore size and the interfacial tension γ of the solution. When the maximum pore size is 0.5 μm, the capillary pressure is $\sim 3 \times 10^5$ Pa at γ = 70 mN/m. The cell is placed in a thermostating device, mounted on the microscope table. Thus the film can be monitored and measured photometrically in reflected light. The apparatus is placed in a special anti-vibration table in a thermostated room. In order to eliminate parasitic stray light, special diaphragms for the falling and reflected light are employed. The reflected light enters the photomultiplier and its signal is amplified and registered by the computer recorder. The regulation of the capillary pressure is achieved by a special membrane pump which allows a gradual and reversible change in the pressure p in the closed cell. The pump and the manometer are placed close to the measuring cell and are connected to it by thick wall tubing, thus ensuring a good thermostating.

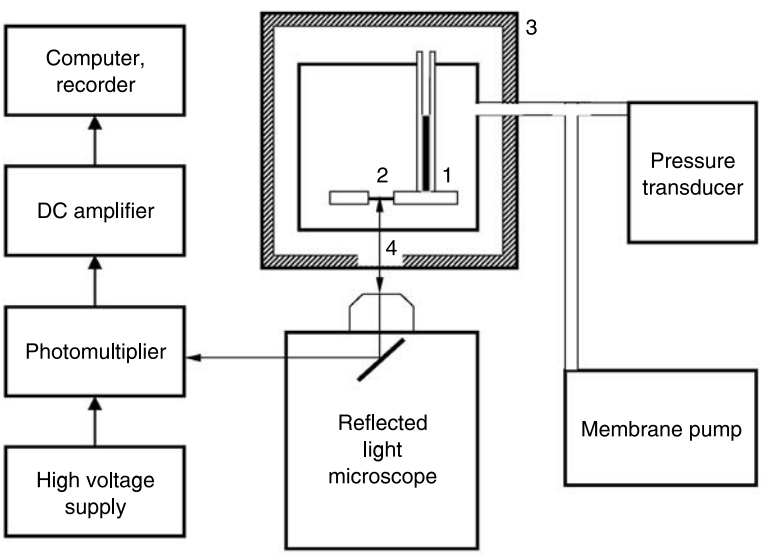

FIGURE 3.7 Block scheme of the thin liquid film–pressure balance technique: 1 is the measuring porous plate cell (cf. Figure 3.3(B)); 2 is the microscopic emulsion or foam film; 3 is a thermostating device; 4 is a plane-parallel glass window.

The thin liquid film–pressure balance technique has been used by a number of researchers who introduced several technical improvements. For example, values of Π less than 100 Pa prove much more difficult to measure, so there should be entire conformity with the equation giving the balance of pressures acting in the film [22] and the geometry of the measuring cell:

$$\Pi = p - p_{\mathrm{r}} + \frac{2\gamma}{r} - \Delta\rho g h_{\mathrm{c}} \tag{3.5}$$

where p_{r} is the external reference pressure; r is the radius of the capillary tube; $\Delta\rho$ is the density difference between the adjacent liquid (or gas) and the surfactant solution from which the film is formed; h_{c} is the height of the solution in the capillary tube above the film.

3.2.5 Measurement of the Contact Angles

The microscopic emulsion or foam film's experimental techniques are used for determination of two other important thermodynamic characteristics of the films: the *contact angle* α_o appearing at the contact of the film with the bulk solution from which it is formed and the *film tension* γ^{f} related to it. Two methods for the measurement of α_o have been developed: a topographic method and a film expansion method [23,24]. The topographic method is most suitable for small contact angles and is used in the study of black films of thickness 6 to 8 nm. This technique is based on the measurement of the radii of the interference Newton rings when the film is observed in a reflected monochromatic light (Figure 3.8). Knowing the film thickness, the contact angle is calculated according to:

$$\mathrm{tg}^2\alpha_o = B^2 - 4A\,(C - h/2) \tag{3.6}$$

where $A = \dfrac{l}{2x_1x_2}\dfrac{2x_1 - x_2}{x_2 - x_1}$; $\quad B = \dfrac{l}{2x_1x_2}\dfrac{x_2^2 - 2x_1}{x_2 - x_1}$; $\quad C = \dfrac{l}{2}$; $\quad l = \dfrac{\lambda}{4n}$

x_1 is the distance between the first and the second Newton rings; x_2 is the distance between the first and the third Newton rings; λ is the light wavelength; n is the refractive index of the film liquid; h is the equilibrium thickness of the film. The applicability of the topographic method can be extended by using an approximated solution of the Laplace equation. Here it is necessary to measure the radius r_k of the k-th Newton ring of the meniscus surrounding the film, and the thickness at which this ring emerges.

The expansion method allows accurate determination of larger contact angles and is suitable for studying Newton black films of thickness about 5 nm. It is based on the ratio between the parameters of the thicker film (r_1 and α_1) and the black film, which results from the thicker film at constant volume of the meniscus. An equilibrium black film of radius r_2 and contact angle $\alpha_2 = \alpha_o$ is formed from the initial non-equilibrium thicker film having parameters r_1 and $\alpha_1 = 0$ during its "expansion" at $V = \mathrm{const}$. The value of α_o can be determined from the experimentally measured values of r_1, r_2, α_1, and R (the tube radius) according to the formula

$$V = \frac{R}{3}E - RuE\,(R + 2/3u) + RuF\,(R + 1/3u) - \frac{r}{3}\sqrt{\left(r^2 - u^2\right)\left(R^2 - r^2\right)} \tag{3.7}$$

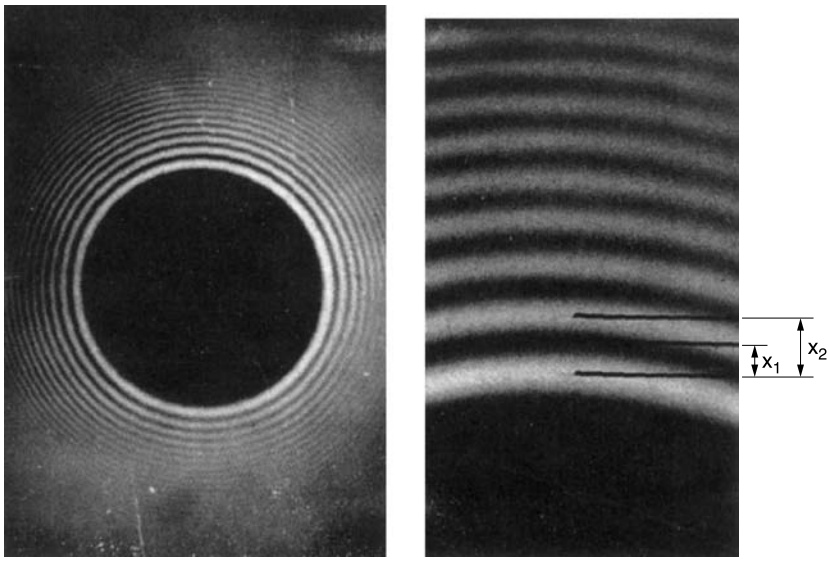

FIGURE 3.8 (a) Microscopic common black film, magnification ~300 times, (b) a segment of its meniscus, additionally enlarged. CBF from 0.277 mM Na dodecylsulphate + 0.2 M NaCl aqueous solution. x_1 and x_2 are the distances between the interference rings. (From T. Kolarov, A. Scheludko, and D. Exerova, *Annuaire Univ. Sofia, Fac. Chim.* 62: 75 (1967–68).)

where $E(\varphi, k^2)$ and $F(\varphi, k^2)$ are elliptic integrals of second and first order and

$$\varphi = \arcsin\sqrt{\frac{R^2 - r^2}{R^2 - u^2}}, \quad k = \frac{R^2 - u^2}{R^2} \quad \text{at} \quad u = \frac{R\sin\alpha_o - r}{R - r\sin\alpha_o}$$

The contact angles can be determined also by the technique of *floating lens* [25], which is widely used in the study of emulsion black films from hydrocarbons in aqueous medium.

There is a simple relation (see Section 3.4) between α_o and γ^f at equilibrium:

$$\gamma^f = 2\gamma\cos\alpha_o \tag{3.8}$$

Hence the film tension is often determined from experimental data about α_o and γ for a given emulsion or foam film.

Certainly the great variety of experimental techniques can not be described in this short section. Besides many variants of the methods reviewed above, there are also other original methods for studying specific aspects of the behavior and properties of thin liquid films.

3.3 THINNING AND RUPTURE OF THIN LIQUID FILMS; BLACK SPOT FORMATION

When a liquid film is formed from a bulk liquid phase α in a surrounding liquid (or gas) β, it is initially a thick liquid film. It becomes a thin liquid film as a result of the *process of thinning* under the driving force $\Delta p = p^\beta - p^\alpha$. This pressure difference can be: the capillary pressure

of the meniscus, a hydrostatic pressure difference, a Δp created by experimental device, etc. An equilibrium thin liquid film is obtained only if Δp is counterbalanced by a positive disjoining pressure Π. However, when Π remains lower than Δp or it is even negative, no equilibrium can be established. The process of thinning leads to either *film rupture* or to jump-like formation of a much thinner *black film* stabilized by enough high positive Π.

The processes film thinning, film rupture, and jump-like formation of black film are the most important non-equilibrium behavior of the thin liquid films. In this section the non-equilibrium properties are considered only for microscopic, circular, horizontal, emulsion, or foam films, surrounded by double-concave meniscus. Such films are obtained in the cylindrical holder of the Scheludko–Exerowa cell (Figure 3.3) and obviously they have a cylindrical symmetry. Microscopic films offer certain advantages with respect to treatment and investigation under strictly defined conditions.

3.3.1 Kinetics of Thinning of Plane-Parallel Liquid Films

An important factor determining the kinetics of thinning of thin liquid films is their anisodiametricity, i.e., their radii are much larger than their thickness, $r \gg h$. Two quantities are introduced for quantitative description of the kinetics of thinning: the lifetime τ of thinning and the rate v of film thinning, defined according to the relations

$$\tau = \int_{h_0}^{h_{cr}} \frac{dh}{v}; \quad v = -\frac{dh}{dt} \tag{3.9}$$

where h_0 is the initial thickness; h_{cr} is the critical thickness at which the film ruptures; t is time.

Let us first consider the kinetics of thinning of plane-parallel, circular films with tangentially immobile interfaces. This is the case of the high degree of tangential blocking of the fluid film's interfaces by a surfactant adsorption layer. Under such conditions the hydrodynamics of thin liquid films is very well described by the Reynolds lubrication theory [26] leading to the well known Stephan–Reynolds relation [27] for the rate v_{Re} of thinning/thickening of a liquid layer of thickness h and viscosity η between two solid circular plates of radius r under a pressure drop Δp

$$-\frac{dh}{dt} = \frac{2h^3 \Delta p}{3\eta r^2} \equiv v_{Re} \tag{3.10}$$

Equation 3.10 was first applied for the kinetics of thinning of circular, horizontal, microscopic liquid films by Scheludko [28]. In his interpretation the pressure drop $\Delta p = \Delta p_c - \Pi$ represents the difference between the capillary pressure Δp_c of the meniscus and the disjoining pressure Π in the film. Thus,

$$\frac{dh^{-2}}{dt} = a\Delta p, \qquad a = \frac{4}{3\eta r^2} \tag{3.11}$$

Since the interfaces of emulsion or foam films considered here are far from rigid and in some cases can deviate considerably from the requirements of the lubrication theory, the applicability of Equation 3.11 to the process of thinning imposes the requirements: (1) viscosity η should not

depend on film thickness; (2) interfaces should be tangentially immobile (zero surface velocity); (3) film interfaces should remain plane-parallel (should not deform); (4) capillary pressure Δp_c of the meniscus should not be affected by film thinning.

There are neither theoretical nor experimental data indicating that there is a dependence of bulk viscosity on film thickness h within the range of 0.01 to 1 μm [29]. One specific feature that distinguishes emulsion films from foam films and films between solid interfaces is the coupling of fluid motion in the adjacent phases. This interdependence of the flows is closely related to the mobility of the liquid/liquid interfaces. The latter is determined by two major factors: (1) the relative viscosity of the droplets η_d and of the film η; and (2) the presence of surfactants.

At close separations between the liquid droplets, the impact of the viscosity factor [30] $\bar{\eta} = \eta_d/\eta$ is modified due to the hindered outflow in the thin liquid film. In flow characteristics, it appears always in a combination with the geometry of the emulsion film (h, the film thickness, and r, the radius of the film) in the form of the hydrodynamic factor $f_h = \bar{\eta}(h/r)$. The rate of film thinning might then be estimated by the following scaling relation [31]:

$$\frac{v}{v_{Re}} \approx \frac{1 + f_h}{(1 + f_h)\left(\frac{h}{r}\right)^2 + f_h} \tag{3.12}$$

The specifications for the cases of emulsion and foam films are

$$\frac{v}{v_{Re}} \Rightarrow 1 + \frac{1}{f_h} \tag{3.12'}$$

for emulsion films, and

$$\frac{v}{v_{Re}} \Rightarrow \left(\frac{r}{h}\right)^2 \tag{3.12''}$$

for foam films. The above equations show that in pure systems the viscosity ratio cannot sustain the pressure drop Δp and the films are thinning always with a velocity higher than v_{Re}.

The other very important factor for the behavior of the emulsion systems is the presence of surfactants. The most popular observation is the so-called Bancroft rule: "The phase in which the stabilizing agent is more soluble will be the continuous phase." The kinetic aspect of this rule is related to the effect of the surfactant mass transfer on the hydrodynamics of emulsion films. This point of view stems from the physicochemical hydrodynamics [30] and was applied for the specific interactions in emulsion films [32].

The key idea is that at small separations the coupling of the surfactant mass transfer and the fluid motion is modified by the formation of thin emulsion films between the approaching droplets. In certain cases, this results in an enhanced suppression of the tangential mobility of the film interfaces, which is affected considerably by the presence of a surfactant through the Marangoni effect [3]. When the liquid drains from a film stabilized by a surfactant, a gradient of surface tension is created at its interfaces which counterbalances the viscous tensions. This gradient, equivalent to the surfactant adsorption gradient, causes the surfactant mass transfer: diffusion flow from the bulk to the film surface, and surface flow in the direction of the adsorption gradient. The tangential velocity of film interfaces is determined by the surface flow and it is always different from zero, i.e., condition "zero surface velocity" is never fulfilled [33].

This effect might be accounted for as a specification of the interfacial mobility scaling by introducing the so-called Marangoni factor f_c and the most general form of the estimate for the drainage rate of the emulsion film acquires [34] the form of

$$\frac{v}{v_{\mathrm{Re}}} \approx \frac{1 + f_h + f_c}{(1 + f_h + f_c)\left(\frac{h}{r}\right)^2 + f_h + f_c} \approx \frac{1 + f_h + f_c}{f_h + f_c} \tag{3.13}$$

For the majority of the cases of correlation between the flow motion and the surfactant fluxes, both effects, f_h and f_c, act in an autonomous additive manner.

The extensive studies on the coupling of film hydrodynamics and the mass transfer of the surfactant during the drainage process have shown that the only case when there is a surfactant influence on the velocity of thinning is when the surfactant is soluble predominantly in the film phase and f_c acquires the form of

$$f_c = \frac{\frac{\Gamma}{\eta D}\left(\frac{\partial \gamma}{\partial c}\right)}{1 + \frac{D_{\mathrm{s}}}{Dh}\left(\frac{\partial \Gamma}{\partial c}\right)} \tag{3.14}$$

where D, D_{s} are, respectively, the bulk and surface diffusion coefficients of the surfactant; γ is the surface tension. The surfactant might block effectively the fluid interfaces even in the case of foam films. The deviation from Equations 3.10 and 3.13 resulting from Marangoni effect has been experimentally observed and theoretically predicted [35] in the expression

$$\frac{v}{v_{\mathrm{Re}}} = 1 - \left[1 - \frac{2D_{\mathrm{s}}}{Dh}\left(\frac{\partial \Gamma}{\partial c}\right)\right] \frac{3D\eta}{\Gamma\left(\partial \gamma / \partial c\right)} \tag{3.15}$$

The quantity $Ma = |\Gamma(\partial\gamma/\partial c)|/D\eta$ is called the Marangoni number and plays an important role in all transport processes at phase interfaces. Other factors (e.g., surface viscosity) affecting surface mobility of films and, hence, kinetics of their thinning are also analyzed [36]. The general criterion for the validity of the Reynolds equation (lubrication theory equations) for the description of emulsion film hydrodynamics [37] states:

$$\frac{f_h + f_c}{1 + f_h + f_c} > \left(\frac{h}{r}\right)^2 \tag{3.16}$$

Equation 3.15 describes correctly the film's hydrodynamics only when factor Ma has large values – equivalent to small deviation from zero surface velocity. The general analysis of the role of surface mobility on the rate of thinning indicates that at high surface mobility ($Ma < 1$) the hydrodynamics of film thinning changes strongly, thus leading to a deviation from the lubrication approximation, Equation 3.10, i.e., the rate of thinning v strongly increases compared to that of films with immobile surfaces v_{Re} [34]. In the limiting case of completely free surfaces (films without a surfactant) the inertia effect prevails to the viscous one (see also Equation 3.12″).

3.3.2 Deviations from the Plane-Parallel Film During its Thinning

The Reynolds relation (Equation 3.10) requires liquid drainage from the film to follow strictly the axial symmetry between parallel walls. Rigid surfaces ensure such drainage through their non-deformability, while non-equilibrium emulsion or foam films are in fact never plane-parallel. This is determined by the balance between hydrodynamic and capillary pressure. Experimental studies have shown that only microscopic films of radii less than 100 μm retain their quasi-parallel surfaces during thinning, which makes them particularly suitable for model studies. Films of larger radii exhibit significant deviations from the plane-parallel shape which affect both the kinetics of thinning and their stability [38].

Not very large films ($r \geq 100$ μm) keep the axial symmetry of thinning but lose their plane-parallel shape. In the center there forms a typical thickening, known as a *dimple* (thicker lens-like formation), whose periphery is a thinner *barrier ring* (Figure 3.4(a)). The dimple forms spontaneously as a result of the hydrodynamic resistance to thinning in the periphery of the circular liquid film [39,40]. Experimental investigations proved that the rate of thinning is practically equal in both the dimple's center and barrier ring, i.e., the difference in thickness of the thickest and the thinnest domains does not decrease up to the critical thickness of rupture. This leads to an increase in the non-uniformity by thickness. On the other hand the non-uniformity by thickness increases with the increase in film size (film radius) as well. These results can be very useful in the interpretation of the experimental data about the dependence of the rate of film thinning and film lifetime on film radius. The experiments indicate [41] a weaker dependence of τ on r (Figure 3.9) than theoretically predicted by Equations 3.11 and 3.15.

A very interesting, in principle different, phenomenon has been observed at the thinning of microscopic, circular O/W/O emulsion films: spontaneous cyclic formation of a dimple occurs in an emulsion film from aqueous solution of the nonionic surfactant Tween 20 between oil droplets [42]. This phenomenon was described as a *diffusion dimple formation* in contrast to the dimple due to the hydrodynamic resistance to thinning in liquid films. The dimple shifted from the center to the periphery and periodically regenerated. During dimple growth the thickness of the circular, almost plane-parallel portion of the film between the dimple and the meniscus remains approximately constant (no change in the reflected light intensity). Photos of the different periods of a dimple growth are shown in Figure 3.10 and the process is schematically presented in Figure 3.11. An explanation has been suggested related to Marangoni effect of continuous

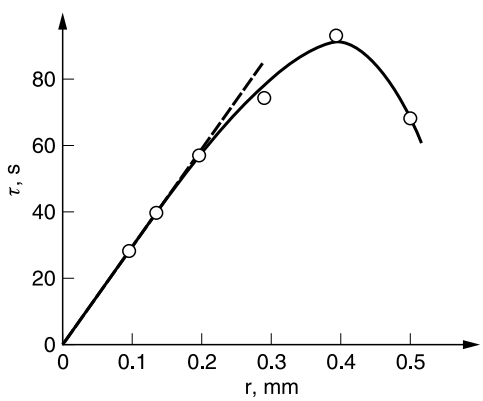

FIGURE 3.9 Film lifetime τ vs. film radius r; foam films from aqueous isovalerianic acid + KCl solution. (From D. Exerova and T. Kolarov, *Annuaire Univ. Sofia, Fac. Chim.* 59: 207 (1964–65).)

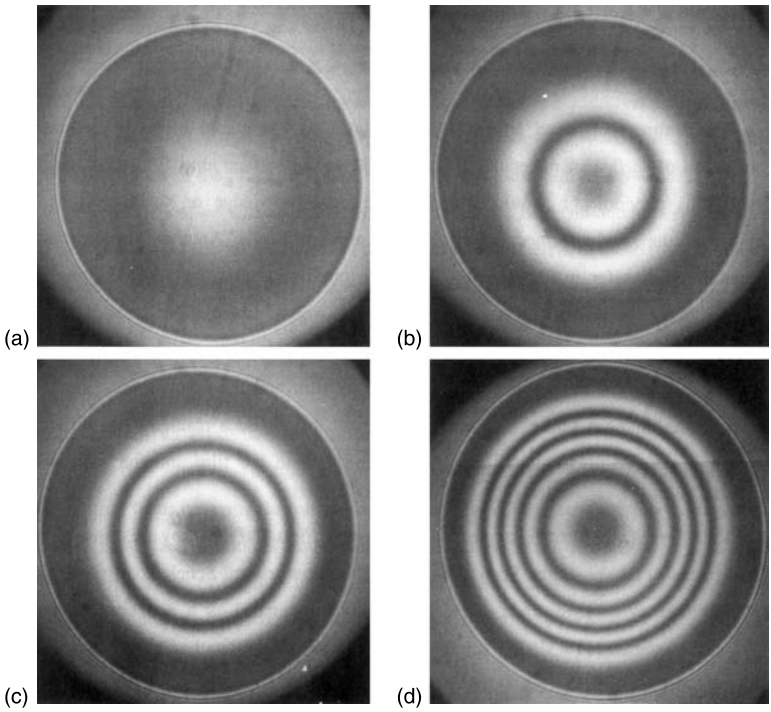

FIGURE 3.10 Four consecutive pictures, (a), (b), (c), and (d), of a spontaneous growth of the dimpling in an aqueous emulsion film with diameter 330 μm. (From O. Velev, T. Gurkov, and R. Borwankar, *J. Colloid Interface Sci.* 159: 497 (1993).)

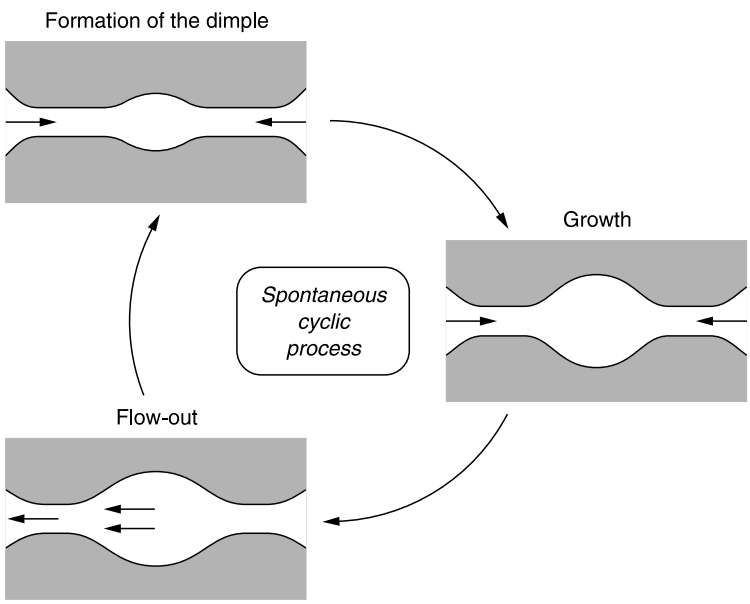

FIGURE 3.11 A cross-section of an emulsion film perpendicular to its interfaces: scheme of the main stages of the spontaneous cyclic process "diffusion dimple formation"; the film and dimple dimensions are not to scale. (From O. Velev, T. Gurkov, and R. Borwankar, *J. Colloid Interface Sci.* 159: 497 (1993).)

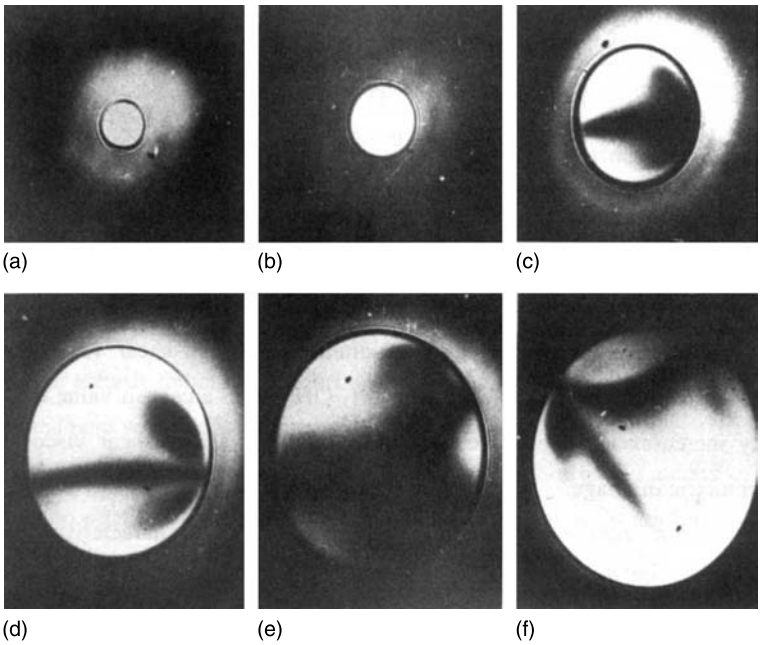

FIGURE 3.12 Six microscopic thin liquid films ($h \sim 100$ nm) with different diameters. Photos **a** and **b**, the smaller films ($r < 100$ μm), are homogeneous by thickness; photos **c**, **d**, **e**, and **f** illustrate the formation of "channels" in larger films ($r > 100$ μm). (From A. Scheludko, *Annuaire Univ. Sofia, Fac. Chim.* 59: 263 (1964–65).)

redistribution of surfactant molecules from the bulk to the surface until film equilibrium is reached. This phenomenon would probably give new understanding of the mechanism of instability in the newly formed emulsion films and emulsions.

During drainage of larger circular, horizontal films ($r > 200$ μm) more complex phenomena have been observed (Figure 3.12). One or more thicker domains form in such films, dividing them into parts [38]. Let us call them "channels." During film thinning the "channels" move and sometimes separate from one end and sink into the meniscus. The axial symmetry of drainage, assumed according to the Reynolds model, is disturbed. At the same time there emerge "centers of thinning" in the film. Such a film drains faster than expected for a homogenous symmetrically draining film of the same size. The complex structure of large films appears spontaneously and, therefore, it corresponds to a more convenient hydrodynamic regime of thinning. The first attempt for theoretical explanation of these effects was based on the idea [43] that the transition from symmetric to asymmetric drainage depends on the presence and the properties of the stabilizing surfactant. A stability criterion for insoluble surfactants was proposed. This criterion was modified for soluble surfactants as well [44].

It seems that the deviations from the plane-parallel shape during the film's thinning are the main reason for considerable differences between the time of thinning measured and calculated from Equation 3.11. At small radii ($r < 200$ μm) and low mobility of film surfaces the experimental and calculated rates of film thinning were very close while at large radii ($r > 200$ μm) the experimentally determined values were ten or more times higher than the calculated ones.

This extremely large difference in the rates and time of thinning cannot be explained only with the tangential mobility of film interfaces (estimated to be 5 to 80%). Moreover, this mobility does not depend on film radius and does not affect the function rate of thinning/radius.

The theoretical model assuming non-deforming film surfaces requires a linear dependence of the rate of thinning on the inverse square of film radius. In all experiments performed the $v(r)$ relation was weaker. These experimental results clearly indicate that Reynolds relation can be applied only to sufficiently small films ($r < 100$ μm), i.e., to films of uniform thickness. Obviously, the main reasons for strong deviations from the theoretical relation should be attributed to the deformations of the film interfaces. With further increase in radius the thinning films lose their axial symmetry and disintegrate into individual subdomains. A theory of the dynamics of large, circular, horizontal films with developed subdomains in them derives an equation [45] about thinning of films nonhomogenous by thickness:

$$v = \frac{1}{6\eta} \sqrt[5]{\frac{h^{12}\Delta p^8}{4\gamma^3 r^4}} \tag{3.17}$$

This equation strongly differs from Reynolds equations (3.10 and 3.11) and has been checked with respect to rate of thinning as a function of film radius (v vs. $r^{-4/5}$). The experimental results are in good agreement with the theoretical prediction. Equation 3.17 holds for large films with strongly expressed nonhomogeneity by thickness. When the film radius decreases the film becomes plane-parallel and its rate of thinning asymptotically satisfies the Reynolds relation. The theory predicts also that the transition between the two regimes of drainage should occur at radius $r^* = 4\sqrt{\gamma h/\Delta p}$. A typical value is $r^* = 50$ μm which agrees well with the experimental observations [46].

3.3.3 Rupture of Thin Liquid Films

One substantial property of the emulsion films is their coalescence stability. The stability of the thin liquid film plays a decisive role. The theory of film rupture was first formulated for the case of foam films. With a slight modification, it is also applicable for emulsion films [47]. The studies show that the true stability of the emulsion films is related to their thermodynamic properties (surface tension, disjoining pressure), exactly as for foam films. The intrinsic coupling of hydrodynamics and mass transfer of surfactants concern the so-called kinetic stability, related to the time evolution of the draining emulsion film. It may be expressed by the interfacial mobility of thin liquid film alone (see Ref. 47, for example). The interfacial mobility of the droplets is important, insofar as it ensures sufficient slowdown of the emulsion film drainage. For higher interface mobility, the drainage velocity is also increased. This increase is also related to the onset of well-defined nonhomogeneities of the film thickness, and, therefore, results in a more rapid coalescence. As a rule, higher interface mobility is observed when surfactants are soluble inside the droplets, or almost equally soluble in the contiguous phases. The basic result is that while for some characteristics (such as lifetime of films) the interfacial mobility is of utmost importance, the thickness of rupture is actually independent on mobility factors.

The study of processes leading to rupture of thin liquid films is useful for understanding the reasons for their stability. The simplest explanation of film rupture involves reaching a thermodynamically unstable state. A typical example of thermodynamically unstable systems are symmetric

thin liquid films in which the van der Waals contribution to disjoining pressure obeys Hamaker's relation, Equation 3.74. Such are films from some aqueous surfactant solutions containing sufficient amount of an electrolyte to suppress the electrostatic component of disjoining pressure as well as films from nonaqueous solutions (see also Section 3.5).

During thinning the thermodynamically unstable films keep their shape in a large thickness range until a rather small thickness is approached, at which the film ruptures. This thickness is called *critical thickness of rupture* h_{cr}. Therefore, the thermodynamic instability is a necessary but not sufficient condition for film instability. There are other factors determining instability which at thicknesses smaller than the critical one cease to act. Two are the possible processes involved in film instability – film thinning while retaining film shape, and film rupture. Which of these is realized when thermodynamic instability is reached requires analysis of the various mechanisms of film rupture.

Contemporary understanding of liquid film rupture is based on the concept of existence of fluctuational waves on liquid surfaces [48]. According to this approach the film is ruptured by unstable waves, i.e., waves the amplitudes of which increase with time. The rupture occurs at the moment when the amplitude Δh or its root mean square value $\sqrt{\overline{(\Delta h)^2}}$ of a certain unstable wave grows up to the order of the film thickness

$$\sqrt{\overline{(\Delta h)^2}} \approx h_{cr} \tag{3.18}$$

The basis of this model has been developed by Scheludko [33,49] who showed that the condition of increase in the amplitude of a wave is equivalent to the condition of increase in local pressure

$$\delta\,(\Delta p_c + \Pi) > 0 \tag{3.19}$$

where

$$\delta \Delta p_c = -\gamma k^2 \Delta h \tag{3.20}$$

is a capillary pressure corresponding to wavelength $\lambda = 2\pi/k$ and amplitude Δh; $\delta\Pi = (\mathrm{d}\Pi/\mathrm{d}h)\Delta h$ is the respective perturbation of disjoining pressure Π. Hence, Equation 3.19 yields

$$k^2 < [\mathrm{d}\Pi/\mathrm{d}h]/\gamma = k_{cr}^2 \tag{3.21}$$

The upper limit k_{cr} of the unstable spectrum range is known as the *Scheludko wave number*.

In thick films ($h > 0.5$ μm) only capillary forces act against the surface deformations, i.e., $\delta\Delta p_c \gg \delta\Pi$ and fluctuation waves are practically stable for the whole wavelength spectrum determined by Equation 3.18. Moreover, the steady state amplitudes of the capillary waves determined from the equipartial law $\sqrt{\overline{(\Delta h)^2}} \approx \sqrt{kT/\gamma}$ at typical conditions ($\gamma \sim 50$ mN m^{-1}; $kT = 4 \times 10^{-21}$ J) have values of the order of $\sqrt{\overline{(\Delta h)^2}} \sim 0.1$ nm, i.e., thick films are not only stable but remain practically unaffected by thermal fluctuations.

In the process of film thinning the interactions due to surface forces in the film become stronger and the attractive components corresponding to the negative disjoining pressure have a destabilizing effect (deepening of amplitude). When only van der Waals forces act in the film, Equations 3.21 and 3.74 give [49] for k_{cr}

$$k_{cr} = \sqrt{\frac{3K_{VW}}{\gamma h^4}} \tag{3.22}$$

Once formed the unstable waves grow until one of them (the fastest) conforms with Equation 3.18 and then the film ruptures. During this time the film thins additionally, depending on the conditions under which it is produced. This kinetic part of the theory of the critical thickness of rupture has been formulated and partially solved by Vrij [50].

An important feature of the kinetics of film rupture is the random character of the process. Here the question is about the correct description of the effect of fluctuations on the evolution of single waves. The further development of the theory gives an expression [46] which seems suitable from an experimental point of view:

$$h_{cr} = \frac{(kT)^{1/10} K_{VW}^{2/5}}{(v\eta)^{1/5} \gamma^{3/10}} \tag{3.23}$$

The experimental data are in good agreement with Equation 3.23. The K_{VW} value recalculated from the experimental data about h_{cr} is very close to the theoretically calculated according to the Lifshitz theory $K_{VW} = 10^{-21}$ J. There are also some corrections introduced in the theory of film rupture later.

Another approach [51] to the rupture of thin liquid films is based on stochastic modeling of this critical transition. Auto-correlation functions for steady state and for thinning liquid films are obtained. A method for calculation of the lifetime τ and h_{cr} of films is introduced. It accounts for the effect of the spatial correlation of waves. The existence of sub-domains leads to decrease in τ and increase in h_{cr}, i.e., increase in the probability for film rupture. Coupling of surface wave dynamics and the rate of drainage v leading to stabilization of thinning films is also accounted for [52].

The mechanism of film rupture proposed by Scheludko and Vrij has stimulated experimental work for determination of h_{cr}. Most successful are those employing the method of microscopic circular thin liquid films with radii $r \sim 100$ μm (Section 3.2). Since rupture is a process with a clearly pronounced random character, reliable measurements of h_{cr} are possible only with microscopic films in which nonfluctuation disturbances are eliminated. The probability character of rupture is illustrated [41] by the curves in Figure 3.13. As can be seen the most probable critical thickness h_{cr} of a film's rupture increases with the increasing film radius, its value being about 30 nm at $r = 0.1$ mm.

3.3.4 Jump-Like Formation of Black Spots in an Emulsion or Foam Film

As shown in the previous section, during thinning, thin liquid films reach a certain critical thickness h_{cr} at which they lose their stability. There are two possibilities: either the film ruptures or a local thinning in the film occurs jump-like. Since at very small thicknesses an emulsion or foam film looks black in reflected light, the jump-like local thinning appearance is called

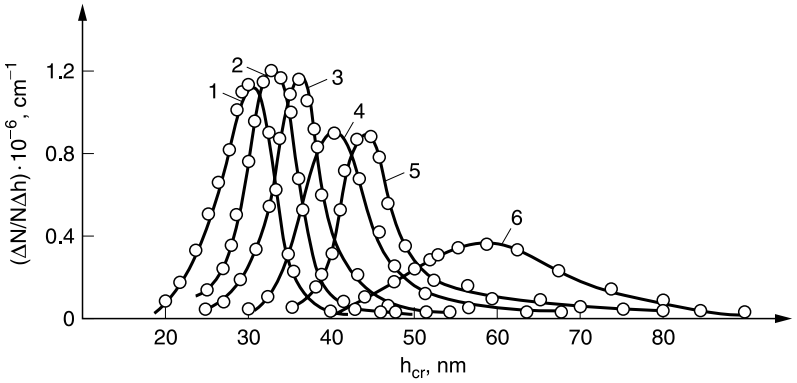

FIGURE 3.13 Distribution curves of the critical thickness of rupture h_{cr}: ΔN is the number of ruptured films with thickness between h and $h + \Delta h$; N is the total number of critical thicknesses measured. Microscopic foam films from isovalerianic acid + KCl aqueous solution with different film radius r. Curve 1: $r = 98$ μm; curve 2: $r = 138$ μm; curve 3: $r = 197$ μm; curve 4: $r = 295$ μm; curve 5: $r = 394$ μm; curve 6: $r = 492$ μm. (From D. Exerova and T. Kolarov, *Annuaire Univ. Sofia, Fac. Chim.* 59: 207 (1964–65).)

formation of *black spots*. The black spot is a very small round area of *black film* which is much thinner than the surrounding area of the unstable thin liquid film. Figure 3.14 shows black spots at different stages of their development.

It appears that Scheludko's theory of rupture of thin liquid films, as well as the new concepts further introduced on that basis (see the previous subsection), are applicable not only to the process of rupture by local thinning but also to the formation of black spots. Hence, black spots can serve to detect the mechanism of local flexion in the film which allows a rough estimation of the fluctuation in wavelength ($\lambda/2$ is about 1 μm). Such a general treatment of instability, including the formation of black spots, can be employed as an additional tool to verify the theory of rupture.

Another important result should also be mentioned: the rupture of unstable films and formation of black spots occur at the same critical thickness: h_{cr} is about 30 nm for films from aqueous surfactant solutions. Emulsion and foam films look gray at this thickness.

What happens in a thinning liquid film when it loses its stability – film rupture at h_{cr} or black spot formation – depends on the surfactant type and concentration in solution. On that basis a new parameter has been introduced [53] for quantitative characterization of the surfactants – emulsion or foam stabilizers. This is the minimal bulk surfactant concentration at which black spots begin to form in the microscopic, unstable, thin liquid film. It is called the *concentration of black spots formation* c_{bl}. This concentration c_{bl} is a very important characteristic of the emulsifiers and foaming agents. Its determination is done by observing emulsion or foam films under a microscope in reflected light. The films are obtained from surfactant solutions with different, gradually increasing, concentration while all other parameters are maintained constant. The lowest concentration at which black spots first appear is c_{bl}.

The concentrations c_{bl} at which various kinds of surfactants ensure formation of stable towards rupture films can be very different depending on the nature of the surfactant molecule. Within a homologous series there is a regular change in c_{bl} – the c_{bl} values decrease with increasing chain length of the molecule. On the other hand c_{bl} is a function of temperature, electrolyte content,

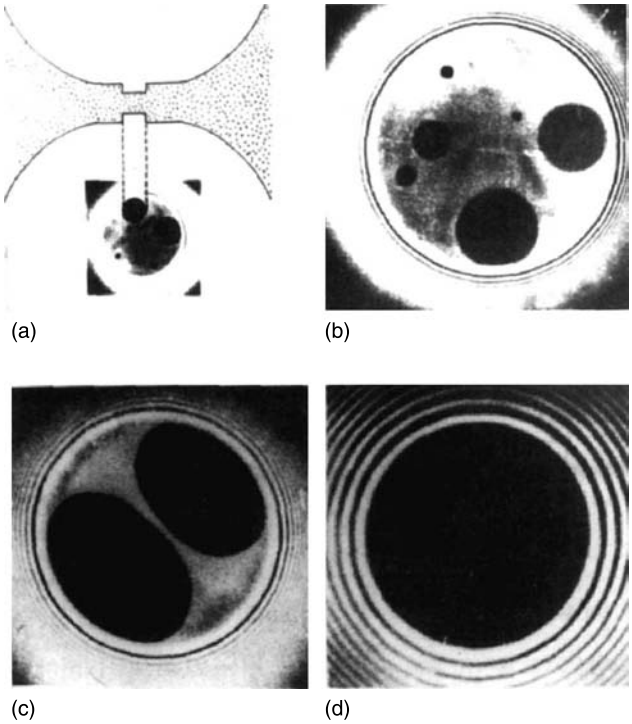

FIGURE 3.14 Formation of black spots and black film in a thicker unstable microscopic liquid film. (a) A schema of the thin black spot in the thicker film; (b) and (c) the growth and coalescence of black spots; (d) the end of the process: the entire film is black. (From D. Exerowa, D. Kashchiev, and D. Platikanov, *Adv. Colloid Polymer Sci.* 40: 201 (1992).)

pH, and presence of other surfactants in the solution. For emulsion films the nature of the second liquid phase also influences c_{bl}. That is why c_{bl} should be determined at standard values of all these parameters.

After the jump-like formation of the black spots, they expand, merge, and at the end the whole film area is occupied by the black film (Figure 3.14). The kinetics of expansion of the black spots in the gray film is also considered. The characteristic concentration c_{bl}, which is a specific for each surfactant parameter, is also important for the emulsion, respectively foam, stability.

3.4 THERMODYNAMICS OF THIN EMULSION AND FOAM FILMS

By definition a thin liquid film is a liquid phase with very small thickness, so that there is no liquid inside the film with the bulk properties of the liquid phase α from which the film has been formed (Figure 3.1). Most of the physical properties vary along the z-axis normal to the film. Hence the thin liquid film is a typical *small* thermodynamic phase. The thermodynamic description of such a system is based, according to Gibbs, on a simplified model. The differences between the values of physical quantities of the model and of the real system are introduced as excess quantities.

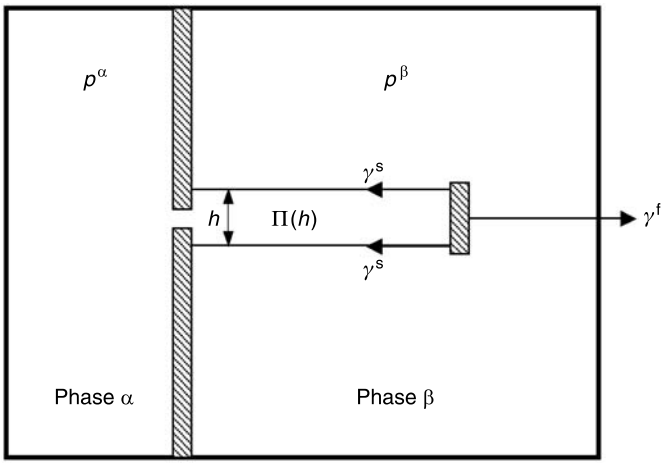

FIGURE 3.15 Scheme of a symmetric plane-parallel thin liquid film (emulsion or foam film) in a frame formed from the liquid phase α and surrounded by the fluid phase β.

In this section a thermodynamic analysis is presented for a symmetric, plane-parallel, horizontal thin liquid film with fluid interfaces. The thermodynamic analysis is developed [54] using only the *model with two Gibbs dividing planes*. It seems that this thermodynamic approach is most convenient for interpretation of the experimental results.

3.4.1 The Simplified Film Model

The entire thermodynamic system (Figure 3.15) consists of: (1) the liquid phase α, in general a multi-component solution; (2) the phase β, either liquid, immiscible with the liquid α (in the case of an emulsion film) or gas (in the case of a foam film); (3) the small phase f, a thin liquid film formed from and connected with the liquid phase α. The thin liquid film is drawn out in a solid frame; the solid material of the vessel walls and the frame is not soluble in phases α and β. The following simplifications are accepted in the film model:

- The Plateau borders, respectively the menisci, at the film contact with the solid walls are neglected. The transition film/meniscus/bulk liquid will be considered later.
- Both interfaces between the film and phase β are replaced by two parallel, horizontal Gibbs dividing planes. The whole space outside the dividing planes is filled by fluid with the bulk properties of phase β.
- The space between the dividing planes is filled by liquid with the bulk properties of the reference phase α.
- The distance h between the dividing planes is defined as thermodynamic thickness h of the thin liquid film.

3.4.2 Mechanical Equilibrium of a Thin Emulsion or Foam Film

Initially a thick liquid film is drawn by the frame from the liquid phase α. It can wear thin only if $p^{\alpha} < p^{\beta}$; the pressure difference $\Delta p = p^{\beta} - p^{\alpha}$ is the driving force for the film thinning.

Why an equilibrium thin liquid film can be obtained at the end of the process of thinning if $\Delta p = \text{constant}$?

The pressure p in an isotropic bulk fluid phase (like phases α and β) is the same everywhere – the Pascal's law. The following components of the pressure tensor are identical:

$$p_{xx} = p_{yy} = p_{zz} = p \tag{3.24}$$

This is not the case of a real interfacial layer as well as a real thin liquid film (Figure 3.1). There only the component p_{zz} of the pressure tensor normal to the film (or single interface) remains constant, while the components parallel to the film (or single interface) are functions of z:

$$p_{zz} = p_{\mathrm{n}} = \text{constant} \tag{3.25}$$

$$p_{xx} = p_{yy} = p_{\mathrm{t}}(z) \tag{3.26}$$

As a result the *interfacial tension* γ arises at each interface between two bulk phases, its mechanical definition being the Bakker's formula:

$$\gamma = \int_{-\infty}^{+\infty} [p_{\mathrm{n}} - p_{\mathrm{t}}(z)]\,\mathrm{d}z = \int_{-\infty}^{+\infty} \left[p^{\beta} - p_{\mathrm{t}}(z)\right]\mathrm{d}z \tag{3.27}$$

The thin liquid film, just as an interface, is anisotropic along the z-axis (Figure 3.1) and by analogy the *film tension* γ^{f} (Figure 3.15) can be defined by the same expression:

$$\gamma^{\mathrm{f}} = \int_{-\infty}^{+\infty} \left[p^{\beta} - p_{\mathrm{t}}(z)\right]\mathrm{d}z \tag{3.28}$$

Here the integration is carried out from the bulk of phase β over the entire film up to the bulk of phase β on the other film side. The film tension is (like the interfacial tension) a force per unit length acting tangential to a surface which is called *surface of tension* of the thin liquid film. In the case of a symmetric, plane-parallel film the surface of tension coincides with the mid-plane of the film. The property film tension of the thin liquid film requires that an external force per unit length γ^{f} has to pull the frame with the film at equilibrium (Figure 3.15).

It is also possible to introduce on the base of the simplified film model (described in the previous subsection) a *surface (interfacial) tension of the film* γ^{s}. Its mechanical definition [11] is given by the equation

$$\gamma^{\mathrm{s}} = \int_{0}^{h/2} \left[p^{\alpha} - p_{\mathrm{t}}(z)\right]\mathrm{d}z + \int_{h/2}^{\infty} \left[p^{\beta} - p_{\mathrm{t}}(z)\right]\mathrm{d}z \tag{3.29}$$

In Equation 3.29 h is the thermodynamic film thickness, i.e., the distance between the two Gibbs dividing planes. Hence γ^{s} depends on the location of the dividing planes, in contrast to the surface (interfacial) tension γ between two bulk phases, which is independent of the location of the single dividing plane. Both γ^{s} and γ^{f} determine the mechanical equilibrium of the film in *tangential* direction.

We shall consider now the mechanical equilibrium of the film in *normal* direction. In the simplified film model the space between the two dividing planes is filled by liquid with pressure p^{α} of the reference phase α (Figure 3.15). The film is thinning because of the pressure difference $\Delta p = p^{\beta} - p^{\alpha}$. Obviously at equilibrium Δp must be balanced by any additional pressure. This pressure, due to the action of surface forces in the film (or pair interactions between the adjacent phases β through the film), has been introduced as *disjoining pressure* Π. Its mechanical definition [55] is given by

$$\Pi = p_{\mathrm{n}} - p^{\alpha} \tag{3.30}$$

i.e., the disjoining pressure is the difference between the normal component of the film's pressure tensor (which is constant) and the pressure in the reference phase α. Taking into account that

$$\Delta p = p^{\beta} - p^{\alpha}, \quad p^{\beta} = p_{\mathrm{n}} \tag{3.31}$$

it follows for symmetric, plane-parallel, horizontal thin liquid films

$$\Pi = \Delta p \tag{3.32}$$

Equation 3.32 is the condition for mechanical equilibrium of the film in normal direction. Positive Π means repulsion between the two film interfaces, i.e., both interfaces are "disjoined" by the interactions due to surface forces. The resultant of all interactions per unit film area is actually Π. It balances the applied external pressure difference Δp. For a plane-parallel, horizontal, real thin liquid film, which contacts trough a Plateau border the frame wall, Δp is the *capillary pressure* at the curved surface of the corresponding meniscus.

Equation 3.28 can be transformed into

$$\begin{aligned}\gamma^{\mathrm{f}} &= 2\int_0^{\infty}\left[p^{\beta} - p_{\mathrm{t}}(z)\right]\mathrm{d}z = 2\int_0^{h/2}\left[p^{\beta} - p_{\mathrm{t}}(z)\right]\mathrm{d}z + 2\int_{h/2}^{\infty}\left[p^{\beta} - p_{\mathrm{t}}(z)\right]\mathrm{d}z \\ &= 2\int_0^{h/2}(p^{\beta} - p^{\alpha})\mathrm{d}z + 2\int_0^{h/2}\left[p^{\alpha} - p_{\mathrm{t}}(z)\right]\mathrm{d}z + 2\int_{h/2}^{\infty}\left[p^{\beta} - p_{\mathrm{t}}(z)\right]\mathrm{d}z\end{aligned} \tag{3.33}$$

The combination of Equation 3.33 with Equations 3.29, 3.31, and 3.32 gives [56]

$$\gamma^{\mathrm{f}} = 2\gamma^{\mathrm{s}} + \Pi h \tag{3.34}$$

This is a very important relation between film tension γ^{f}, surface tension of the film γ^{s}, disjoining pressure Π, and film thickness h – the most important thermodynamic characteristics of a thin liquid film.

3.4.3 Fundamental Thermodynamic Equations of a Thin Liquid Film

The fundamental thermodynamic equation for the internal energy U^f of the thin liquid film (Figure 3.15) follows directly from the First and Second Laws:

$$dU^f = TdS^f - p^\beta dV^f + \gamma^f dA^f + \sum_i \mu_i dn_i^f \tag{3.35}$$

Here and further all superscripts denote the phase to which the respective quantity belongs. The first term to the right reflects the heat reversibly transferred to the film from outside, S^f being the entropy of the film. The second term is the volume work done on the film by its surroundings, V^f being the film volume; note that this work is done by the pressure p^β which is an external pressure with respect to the film. The work done for reversible increase of the film area A^f is given by the third term to the right. The last term gives the "chemical" work done when the moles n_i^f of each component in the film are increased. The temperature T and the chemical potential μ_i of each component i are considered constant in all three phases f, α, and β (Figure 3.15). Using the Legendre transformations we can obtain the fundamental thermodynamic equations for the Helmholtz free energy F^f and for the Gibbs energy G^f of the thin liquid film:

$$dF^f = -S^f dT - p^\beta dV^f + \gamma^f dA^f + \sum_i \mu_i dn_i^f \tag{3.36}$$

$$dG^f = -S^f dT + V^f dp^\beta + \gamma^f dA^f + \sum_i \mu_i dn_i^f \tag{3.36'}$$

The integration of Equation 3.35 according to Euler's theorem at constant T, p^β, γ^f, and μ_i gives the total internal energy U^f of the thin liquid film:

$$U^f = TS^f - p^\beta V^f + \gamma^f A^f + \sum_i \mu_i n_i^f \tag{3.37}$$

The differentiation of Equation 3.37 gives

$$\begin{aligned} dU^f = {} & TdS^f + S^f dT - p^\beta dV^f - V^f dp^\beta + \gamma^f dA^f + A^f d\gamma^f \\ & + \sum_i \mu_i dn_i^f + \sum_i n_i^f d\mu_i \end{aligned} \tag{3.38}$$

The combination of Equations 3.38 and 3.35 leads to the very important Gibbs–Duhem relation of the thin liquid film:

$$S^f dT - V^f dp^\beta + A^f d\gamma^f + \sum_i n_i^f d\mu_i = 0 \tag{3.39}$$

The Gibbs–Duhem relation expressed per unit film area reads:

$$\begin{aligned} & d\gamma^f = -S_A^f dT + h dp^\beta - \sum_i \Gamma_i^f d\mu_i \\ & \frac{V^f}{A^f} = h, \quad \frac{S^f}{A^f} = S_A^f, \quad \frac{n_i^f}{A^f} = \Gamma_i^f \end{aligned} \tag{3.40}$$

All fundamental equations as well as Gibbs–Duhem relations considered above are the most general thermodynamic equations of the thin liquid film. They do not depend on the film model chosen since the extensive film properties have not been specified yet. These equations are valid for symmetric, horizontal, plane-parallel films with fluid interfaces under the condition that the Plateau borders, respectively, the menisci, at the film contact with phase α, or the solid walls are neglected. However, the equations can be used also in the more complicated system which includes Plateau borders, menisci, etc. if the thermodynamic state of all parts of the system, except the film itself, is kept constant.

3.4.4 Thermodynamic Approach with Two Gibbs Dividing Planes

According to this model the thin liquid film consists of two parallel mathematical planes (Gibbs dividing planes), the space between them being filled by liquid with the bulk properties of the reference phase α; the space outside the dividing planes is filled by fluid with the bulk properties of phase β (Figure 3.15). The differences between the extensive thermodynamic properties of the model and of the real film are introduced as surface excess quantities. So the surface excess internal energy U_A^{sf} of the film per unit area of each film surface is presented as

$$U_A^{\mathrm{sf}} = \int_0^{h/2} \left[U_v(z) - U_v^{\alpha}\right] \mathrm{d}z + \int_{h/2}^{\infty} \left[U_v(z) - U_v^{\beta}\right] \mathrm{d}z \tag{3.41}$$

In Equation 3.41 U_v^{α} and U_v^{β} are the volume densities of the internal energy in the homogeneous bulk phases α and β respectively; $U_v(z)$ is the volume density of the internal energy in the inhomogeneous real film. The excess surface concentration Γ_i^{sf} of each component i in the film, per unit area of each film surface, is given by

$$\Gamma_i^{\mathrm{sf}} = \int_0^{h/2} \left[n_{\mathrm{vi}}(z) - n_{\mathrm{vi}}^{\alpha}\right] \mathrm{d}z + \int_{h/2}^{\infty} \left[n_{\mathrm{vi}}(z) - n_{\mathrm{vi}}^{\beta}\right] \mathrm{d}z \tag{3.42}$$

n_{vi}^{α} and n_{vi}^{β} being the volume densities of each component i in the homogeneous bulk phases α and β respectively and $n_{\mathrm{vi}}(z)$ the volume density of each component i in the inhomogeneous real film.

The surface excess quantities as defined by Equations 3.41 and 3.42, as well as other surface excess extensive properties of the film, depend on the location of the Gibbs dividing planes. Just as in the case of a single interface different conditions which determine the dividing plane location can be accepted. The best possibility is when the same condition determines the location both of a single dividing plane between the phases α and β and of the film dividing planes. So the surface excess properties of the film and of the single interface can directly be compared with each other. Most often the condition $\Gamma_1^{\mathrm{sf}} = 0$ is used, i.e., the surface excess of component 1 in the film is zero, component 1 being the liquid which is solvent in phase α.

According to the simplified model the total thin liquid film consists of two Gibbs dividing planes and a volume part filled by liquid with the bulk properties of the reference phase α. Hence the total extensive properties of the film can be obtained as a sum of the doubled surface excess quantity plus the corresponding extensive quantity of the volume part of the film. So the internal

energy U^{f} of the total film is presented as

$$U^{\mathrm{f}} = 2U^{\mathrm{sf}} + U^{\alpha\mathrm{f}} = A^{\mathrm{f}}\left(2U_A^{\mathrm{sf}} + hU_v^{\alpha}\right) \tag{3.43}$$

where U^{sf} is the surface excess internal energy at one dividing plane and $U^{\alpha\mathrm{f}}$, the internal energy of the volume part of the total film. The total amount n_i^{f} of each component i in the film is expressed by

$$n_i^{\mathrm{f}} = 2n_i^{\mathrm{sf}} + n_i^{\alpha\mathrm{f}} = A^{\mathrm{f}}\left(2\Gamma_i^{\mathrm{sf}} + hn_{\mathrm{vi}}^{\alpha}\right) \tag{3.44}$$

n_i^{sf} being the surface excess amount of each component i in the film and $n_i^{\alpha\mathrm{f}}$ the amount of component i in the volume part of the total film.

If we accept that the surface excess of component 1 in the film is zero, as a condition which determines the location of the Gibbs dividing planes, we obtain from Equation 3.44 an equation which determines the thermodynamic film thickness h:

$$n_1^{\mathrm{f}} = A^{\mathrm{f}} h n_{\mathrm{v1}}^{\alpha}, \quad \Gamma_1^{\mathrm{sf}} = 0 \tag{3.45}$$

$$h = \frac{n_1^{\mathrm{f}}}{\mathrm{A}^{\mathrm{f}} n_{\mathrm{v1}}^{\alpha}} \tag{3.46}$$

According to Equation 3.46 the thermodynamic film thickness h is equal to the thickness of a layer of the solution in phase α, which contains the same amount of component 1 as the film. The real emulsion (or foam) films are usually stabilized by dense surfactant adsorption layers at both interfaces. That means the thermodynamic film thickness is closer to the thickness of the inner liquid layer of the film, rather than to the whole film thickness. However, the surfactant molecules can be very different and the film structure as well. Hence the comparison of the thermodynamic and the real film thickness should be done for each system separately. In general the physical film thickness is usually larger than the thermodynamic thickness determined under condition 3.45.

Equation 3.43 after differentiation can be transformed into

$$2\mathrm{d}U^{\mathrm{sf}} = \mathrm{d}U^{\mathrm{f}} - \mathrm{d}U^{\alpha\mathrm{f}} \tag{3.47}$$

The fundamental thermodynamic equation for the internal energy $U^{\alpha\mathrm{f}}$ of the volume part of the thin liquid film reads

$$\mathrm{d}U^{\alpha\mathrm{f}} = T\mathrm{d}S^{\alpha\mathrm{f}} - p^{\alpha}\mathrm{d}V^{\mathrm{f}} + \sum_i \mu_i \mathrm{d}n_i^{\alpha\mathrm{f}} \tag{3.48}$$

The combination of Equation 3.47 with 3.35 and 3.48, taking into account Equations 3.31, 3.32, and 3.44, and the relation $S^{\mathrm{f}} = 2S^{\mathrm{sf}} + S^{\alpha\mathrm{f}}$, gives

$$2\mathrm{d}U^{\mathrm{sf}} = 2T\mathrm{d}S^{\mathrm{sf}} - \Pi\mathrm{d}V^{\mathrm{f}} + \gamma^{\mathrm{f}}\mathrm{d}A^{\mathrm{f}} + 2\sum \mu_i \mathrm{d}n_i^{\mathrm{sf}} \tag{3.49}$$

This is the fundamental thermodynamic equation for the surface excess of the internal energy of the film. Following the usual procedure, the corresponding important Gibbs–Duhem relation of

the Gibbs dividing planes of the film can be obtained

$$2S^{sf}\mathrm{d}T - V^{f}\mathrm{d}\Pi + A^{f}\mathrm{d}\gamma^{f} + 2\sum n_i^{sf}\mathrm{d}\mu_i = 0 \tag{3.50}$$

which, assigned to unit film area, reads

$$\mathrm{d}\gamma^{f} = -2S_A^{sf}\mathrm{d}T + h\mathrm{d}\Pi - 2\sum_i \Gamma_i^{sf}\mathrm{d}\mu_i \tag{3.51}$$

The substitution of Equation 3.34 into 3.49 leads to another form of the fundamental thermodynamic equation for the surface excess of the internal energy of the film:

$$2\mathrm{d}U^{sf} = 2T\mathrm{d}S^{sf} - \Pi A^{f}\mathrm{d}h + 2\gamma^{s}\mathrm{d}A^{f} + 2\sum \mu_i \mathrm{d}n_i^{sf} \tag{3.52}$$

Respectively, the Gibbs–Duhem relation of the dividing planes of the film takes another form as well:

$$2S^{sf}\mathrm{d}T + \Pi A^{f}\mathrm{d}h + 2A^{f}\mathrm{d}\gamma^{s} + 2\sum n_i^{sf}\mathrm{d}\mu_i = 0 \tag{3.53}$$

or assigned to unit film area:

$$2\mathrm{d}\gamma^{s} = -2S_A^{sf}\mathrm{d}T - \Pi\mathrm{d}h - 2\sum \Gamma_i^{sf}\mathrm{d}\mu_i \tag{3.54}$$

On the basis of both Gibbs–Duhem equations (3.54 and 3.51) very useful relations between the main thermodynamic characteristics (h, Π, γ, γ^{f}, γ^{s}) of the thin liquid film can be obtained. From Equation 3.54 it follows that

$$2\left(\frac{\partial\gamma^{s}}{\partial h}\right)_{T,\mu_i} = -\Pi \tag{3.55}$$

which after integration at constant temperature and all chemical potentials (for thick film $h \to \infty$, $\Pi = 0$, $\gamma^{s} = \gamma$) gives

$$2(\gamma^{s} - \gamma) = -\int_{\infty}^{h} \Pi dh = \Delta F(h)$$

or

$$2\gamma^{s} = 2\gamma + \Delta F(h) \tag{3.56}$$

The quantity $\Delta F(h)$ is usually called *interaction free* (*Helmholtz*) *energy of the film*. Obviously this is the isothermal, reversible work per unit film area done against the disjoining pressure when thinning of a thick film down to a small equilibrium thickness h.

Equation 3.55 shows that when disjoining pressure Π appears due to interactions in the thin liquid film, the surface tension of the film γ^{s} depends on the film thickness and it differs from the surface tension γ of the bulk liquid phase. This result was not accepted by some authors

who claim that one liquid surface (in our case film/transition zone/bulk meniscus) should have everywhere a constant surface tension at equilibrium; otherwise a flow in the liquid surface layer would arise due to the surface tension gradient. It has been shown [57] that this is an apparent contradiction and both approaches – the one assuming variable surface tension and the other based on constant surface tension – are completely equivalent. The apparent differences are due to the simplified thermodynamic approach chosen.

Other similar relations can be obtained from Equation 3.51:

$$\left(\frac{\partial \gamma^{\mathrm{f}}}{\partial \Pi}\right)_{T,\mu_i} = h \tag{3.57}$$

which after integration at constant temperature and all chemical potentials gives

$$\gamma^{\mathrm{f}} = 2\gamma - \int_{\infty}^{h} \Pi \mathrm{d}h + \Pi h$$

or

$$\gamma^{\mathrm{f}} = 2\gamma + \Pi h + \Delta F(h) \tag{3.58}$$

Equation 3.58 can be used to determine the interaction free energy of the film $\Delta F(h)$ from experimental data for γ and γ^{f} (the last two quantities can be directly measured). The product Πh is usually very small since h is extremely small for the so-called *black films* – the case when 2γ and γ^{f} noticeably differ. Then Πh is neglected and $\Delta F(h) \approx \gamma^{\mathrm{f}} - 2\gamma$.

From the fundamental thermodynamic equations (3.52 and 3.49) for the surface excess of the internal energy of the film, using the Legendre transformations we can obtain the corresponding fundamental thermodynamic equations for the surface excess of the Helmholtz free energy of the film:

$$2\mathrm{d}F^{\mathrm{sf}} = -2S^{\mathrm{sf}}\mathrm{d}T - \Pi \mathrm{d}V^{\mathrm{f}} + \gamma^{\mathrm{f}}\mathrm{d}A^{\mathrm{f}} + 2\sum \mu_i \mathrm{d}n_i^{\mathrm{sf}} \tag{3.59}$$

$$2\mathrm{d}F^{\mathrm{sf}} = -2S^{\mathrm{sf}}\mathrm{d}T - \Pi A^{\mathrm{f}}\mathrm{d}h + 2\gamma^{\mathrm{s}}\mathrm{d}A^{\mathrm{f}} + 2\sum \mu_i \mathrm{d}n_i^{\mathrm{sf}} \tag{3.60}$$

A thermodynamic definition of the film tension γ^{f} follows from Equation 3.59:

$$\gamma^{\mathrm{f}} = 2\left(\frac{\partial F^{\mathrm{sf}}}{\partial A^{\mathrm{f}}}\right)_{T,V^{\mathrm{f}},n_i^{\mathrm{sf}}} \tag{3.61}$$

By analogy thermodynamic definitions of the surface tension of the film γ^{s} and of the disjoining pressure Π can be derived from Equation 3.60:

$$\gamma^{\mathrm{s}} = \left(\frac{\partial F^{\mathrm{sf}}}{\partial A^{\mathrm{f}}}\right)_{T,h,n_i^{\mathrm{sf}}} \tag{3.62}$$

$$\Pi = -\frac{2}{A^{\mathrm{f}}}\left(\frac{\partial F^{\mathrm{sf}}}{\partial h}\right)_{T,A^{\mathrm{f}},n_i^{\mathrm{sf}}} \tag{3.63}$$

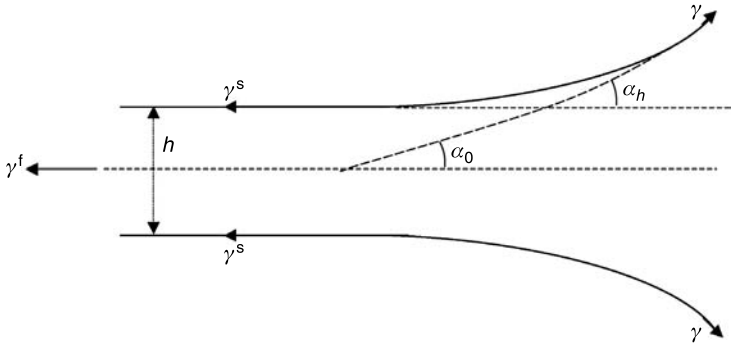

FIGURE 3.16 Scheme of part of a plane-parallel symmetric thin liquid film (left side) connected through a transition zone with a meniscus of the liquid phase α.

Equations 3.61 to 3.63 show that all three quantities characterizing the film, γ^{f}, γ^{s}, and Π, are defined in terms of the surface excess of the Helmholtz free energy, a main feature of the thermodynamic approach with two Gibbs dividing planes.

3.4.5 Contact Between a Thin Emulsion or Foam Film and the Adjacent Bulk Liquid

A thin liquid film is always connected with a bulk liquid phase or with a solid wall through a *Plateau border* – a liquid body with concave interfaces like a meniscus. The Plateau border contains bulk liquid α from which the film has been formed. The contact film/Plateau border is schematically presented in Figure 3.16. On the left side there is a part of the horizontal, plane-parallel, symmetric, thin liquid film (emulsion or foam film) and on the right side, a part of the Plateau border. A *transition zone film/bulk* always exists between them [58]. At equilibrium the disjoining pressure Π acts in the film and the surface tension of the film γ^{s} differs from the interfacial (surface) tension γ of the bulk liquid phase. Both Π and γ^{s} are due to the surface force interactions in the thin liquid film. These interactions operate in the transition zone film/bulk as well, but they decrease with increasing thickness of the transition zone towards the meniscus. This means that both Π and $(\gamma - \gamma^{s})$ gradually decrease along the transition zone in direction from the film to the Plateau border, becoming zero in the bulk liquid.

In a real system the curved meniscus interface gradually becomes a flat film interface and γ gradually turns into γ^{s}. The macroscopic thermodynamic description neglects the presence of a transition zone and assumes an abrupt change of γ (bulk liquid) into γ^{s} (film). This simplified thermodynamic approach requires introduction of two other thermodynamic quantities: the *contact angle film/bulk* and the *line tension* of the contact line. Thus the simplified macroscopic thermodynamic description becomes equivalent to the real system.

In the Plateau border the interfacial (surface) tension of the bulk liquid is γ and the shape of its concave interface is determined by the Laplace equation. If we consider γ constant also in the transition zone and extrapolate the meniscus interface according to Laplace equation towards the film (the dotted curve in Figure 3.16), it intersects the mid-plane of the film (the horizontal dotted straight line). The line of intersection is the *contact line* of the film and the angle between both dotted lines is the *contact angle* α_o [59,60].

If we consider a cylindrical meniscus, i.e., a straight contact line, the balance of forces in tangential direction, taking into account Equation 3.58, is given by

$$\gamma^{\mathrm{f}} = 2\gamma \cos\alpha_0 = 2\gamma + \Pi h + \Delta F(h) \tag{3.64}$$

In the case of a curved contact line (e.g., a round film in a spherical meniscus) the balance of forces reads [61]

$$2\gamma \cos\alpha_0 = \gamma^{\mathrm{f}} + \frac{\kappa}{r^{\mathrm{f}}} \tag{3.65}$$

where κ is the line tension and r^{f} is the radius of curvature of the contact line. The term κ/r^{f} is actually a two-dimensional capillary pressure, a surface pressure difference on both sides of the curved contact line. However, this term is usually very small because of the very small κ value; it should be taken into account at extremely small r^{f} only.

Another definition of the contact angle film/bulk has been introduced as well: the angle α_h between the extrapolated according to Laplace equation meniscus interface towards the film (the dotted curve in Figure 3.16) and the extrapolated surface of the film (the upper horizontal dotted straight line). Obviously the contact angles α_h and α_o are different but this difference is usually very small. In this case the balance of forces in tangential direction (straight contact line), taking into account Equation 3.56, is given by

$$\gamma^{\mathrm{s}} = \gamma \cos\alpha_h, 2\gamma \cos\alpha_h = 2\gamma + \Delta F(h) \tag{3.66}$$

The contact angles α_h and α_o can be measured experimentally. From these experimental values with a measured γ value one can calculate values of the interaction free (Helmholtz) energy $\Delta F(h)$ of the film:

$$\Delta F(h) = -2\gamma(1 - \cos\alpha_h) \tag{3.67}$$

$$\Delta F(h) = -2\gamma(1 - \cos\alpha_0) - \Pi h \tag{3.68}$$

As already noted in the previous section, the term Πh is usually very small. In such a case if we accept that $\Pi h \approx 0$, it follows that $\alpha_h \approx \alpha_o$.

3.5 SURFACE FORCES IN THIN EMULSION AND FOAM FILMS

According to the thermodynamics of the thin liquid films, the most important factor which determines their properties is the interaction between the two film interfaces, i.e., the pair interactions between the two adjacent phases across the liquid film. The thermodynamic quantity *disjoining pressure* Π is a result of these interactions, due to different types of *surface forces* acting in the thin liquid films. The dependence of the disjoining pressure on the film thickness, the so-called *disjoining pressure isotherm*, is closely related with the more general problem of the stability of a disperse system. Hence knowledge about the surface forces in the thin liquid films has developed in connection with the theories of colloid stability, the most important being the theory of Derjaguin, Landau, Verwey, and Overbeek – the DLVO theory [7,8].

Major efforts are directed to understanding the nature and origin of surface forces acting in thin liquid films, including bilayer films. On the other hand explanations are sought for the cases in which the classical DLVO theory contradicts experimental findings. Two categories of

surface forces are usually distinguished: DLVO and non-DLVO surface forces. The *van der Waals molecular interactions* or *dispersion molecular forces* as well as the *electrostatic* or *double layer forces* are called DLVO forces (both long-range forces), the balance of which lays the foundation for the DLVO theory. The non-DLVO forces are of different nature [62,63]. Most important for the symmetric thin liquid films with fluid interfaces (emulsion and foam films) are the *steric surface forces*, long range for macromolecules, short range for small molecules. Theoretical as well as experimental considerations are put forth for the existence of *structural* (*solvation, hydration, or hydrophobic*) *surface forces* in some cases; they originate from modifications in the liquid structure adjacent to the film interfaces. In specific film cases other surface forces could be introduced as well.

The precise direct measurement of surface forces is a subject of current interest, since it provides sufficiently reliable distinction of the forces, along with the elucidation of their mutual influence, their dependence on the distance between the interacting surfaces (the film thickness) in systems of different composition, temperature, etc. All this enables a more critical application of the theories of the known surface forces. On the other hand, the direct measurement of surface forces stimulates theoretical analyses. Surface force measurements in emulsion and foam films, in particular in microscopic films, stabilized with amphiphile molecules (surfactants, phospholipids, polymers), enable the study of these forces at large film thickness, long-range surface forces as well as interaction forces at the formation of a bilayer film. The long-range/short-range interaction transitions, including the reversal transition, are also studied in detail.

3.5.1 DLVO Surface Forces: Theoretical

The dependence of the disjoining pressure Π on film thickness h, the $\Pi(h)$ isotherm, is at the root of the DLVO theory of stability of lyophobic colloids. According to this theory the disjoining pressure in thin liquid films is considered as a sum of an electrostatic component Π_{el} and a van der Waals component Π_{VW}:

$$\Pi = \Pi_{el} + \Pi_{VW} \tag{3.69}$$

A complete analysis of the theory can be found in several monographs (e.g., Refs. 8, 62, and 63). Here, only a few expressions, which are used for interpretation of the experimental results, are presented.

3.5.1.1 Electrostatic Disjoining Pressure

The electrostatic or double layer disjoining pressure is given by the equation:

$$\Pi_{el} = 2cRT(\cosh zy^m - 1) \tag{3.70}$$

with $m = h/2$ and $y^m = F\psi^m/RT$. Here c is the concentration of a symmetric electrolyte of valence z, F is Faraday's constant; ψ^m is the potential at a distance $h/2$ (at the central plane of the symmetric film) which is connected to the potential ψ^0 of the double electric layer at the film/adjacent phase interface through the relation:

$$-\frac{\kappa h}{2} = \int_{y=y^0}^{y=y^m} \frac{z\,dy}{\sqrt{2\,[\cos h(zy) - \cos h(zy^m)]}} \tag{3.71}$$

with

$$y = \frac{F\psi}{RT}, \quad y^0 = \frac{F\psi^0}{RT}$$

and

$$\kappa = \sqrt{F^2 z^2 c/\varepsilon_0 \varepsilon RT} \tag{3.72}$$

where ε is the relative dielectric permittivity and $\varepsilon_0 = 8.854 \times 10^{-12}$ $C^2V^{-1}m^{-1}$ is the dielectric permittivity of free space (vacuum).

An approximated expression of the electrostatic component of disjoining pressure can be derived from Equation 3.70 at small values of ψ^m

$$\Pi_{el} = \frac{64cRT}{z^2}\left[\tanh(zy^0/4)\right]^2 e^{-\kappa h} \tag{3.73}$$

Equation 3.73 is quite adequate for prompt calculations of Π_{el}. For a wide range of ψ^0 and c values, it is necessary to use the more general equations (3.70 and 3.71).

3.5.1.2 van der Waals Disjoining Pressure

Two theories, macroscopic and microscopic, are involved in the calculation of the van der Waals component Π_{VW} of disjoining pressure in thin liquid films. According to the *microscopic theory*, the total interaction force in a flat gap between two semi-infinite phases decreases with distance much slower than the interaction force between two individual molecules. The following expression for the van der Waals component of disjoining pressure in a symmetric film bordering gas or condensed phases is obtained:

$$\Pi_{VW} = -K_{VW}/h^n \tag{3.74}$$

where K_{VW} is the van der Waals–Hamaker constant (introduced by A. Scheludko); $K_{VW}(h) = A(h)/6\pi$, $A(h)$ being the Hamaker constant for symmetric films, a weak function of film thickness. In general $n = 3$; but if a correction for the electromagnetic retardation of dispersion forces is taken into account [64], $n = 4$.

A general formula for calculation of the dispersion molecular interactions in any type of condensed phases has been derived in the *macroscopic theory*. The attraction between bodies results from the existence of a fluctuational electromagnetic field of the substance. If this field is known for a thin liquid film, it is possible to determine the disjoining pressure in it. The more strict macroscopic theory avoids the approximations assumed in the microscopic theory, i.e., additivity of forces; integration; extrapolation of interactions of individual molecules in the gas to interactions in the condensed phase. The macroscopic theory is successfully used for calculation of the dispersion molecular interactions, respectively the $\Pi_{VW}(h)$. Several approximations have been derived since the exact equations are too complicated. A good approximation for symmetric flat films is

$$\Pi_{VW} = -\frac{\hbar}{8\pi^2 h^3}\int_0^\infty \left(\frac{x^2}{2} + x + 1\right) e^{-x} \frac{(\varepsilon_f - \varepsilon)^2}{(\varepsilon_f + \varepsilon)^2} d\omega \tag{3.75}$$

with $x = 2\omega h\varepsilon_f^{1/2}$, ε_f, and ε being the relative dielectric permittivities (functions of the frequency ω) of the film and the adjacent phases respectively; $\hbar$ is Planck's constant divided by 2π. For small film thickness a more simple approximation can be derived:

$$\Pi_{VW} = -\frac{\hbar}{8\pi^2 h^3}\int_0^\infty \frac{(\varepsilon_f - \varepsilon)^2}{(\varepsilon_f + \varepsilon)^2} d\omega \tag{3.76}$$

Another approximation for a foam film with relatively large thickness reads

$$\Pi_{VW} = \frac{\hbar c}{h^4}\frac{\pi^2}{240\sqrt{\varepsilon_0}}\left(\frac{1-\varepsilon_0}{1+\varepsilon_0}\right)^2 \varphi\left(\frac{1}{\varepsilon_0}\right) \tag{3.77}$$

where ε_0 is the static value of the dielectric permittivity of the film; c is the speed of light. Here Π_{VW} is inversely proportional to h^4, similar to the Hamaker's formula which accounts for the electromagnetic retardation of dispersion forces [64].

For practical use of the macroscopic theory equations with empirical constants are also appropriate for calculation of Π_{VW}, for instance [65]

$$\Pi_{VW} = h^{-3}\left[b + (a + ch)/(1 + dh + eh^2)\right] \tag{3.78}$$

where a, b, c, d, and e are empirical constants.

3.5.2 DLVO Surface Forces: Experimental

Quantitative experimental studies of the DVLO surface forces have been performed with microscopic emulsion and foam films. As shown above, the disjoining pressure is given as a sum of Π_{el} and Π_{VW}, i.e., they are considered independent. In the symmetric emulsion or foam film Π_{el} is always positive while Π_{VW} is always negative. In an equilibrium film, the state of which is determined by the action of the positive disjoining pressure, Π can be calculated from the balance of the forces experimentally obtained. When Π is negative, it is possible to use the dynamic method [33] according to which $\Pi(h)$ is calculated using the hydrodynamic equation for the rate of film thinning (see Equation 3.11). During film thinning at $h > \approx 120$ nm the constant capillary pressure only determines the rate of thinning and $1/h^2$ vs time t is a straight line according to Equation 3.11. Below thickness of ≈ 120 nm the disjoining pressure appears and it accelerates or decelerates the liquid outflow. From the experimental $1/h^2(t)$ dependence the pressure drop $\Delta p = \Delta p_c - \Pi$ is calculated and with a known Δp_c value the experimental Π values are determined for different film thickness. This method enables the study of the $\Pi(h)$ isotherm within a large thickness range. It also provides a possibility to verify the different theories of disjoining pressure, including the cases in which Π is always negative and no equilibrium films are formed.

3.5.2.1 Experiments with Foam Films

The first quantitative proof of the DLVO theory has been conducted [66] on a model system – microscopic foam film using the microinterferometric technique (Figures 3.3 and 3.7). Independent studies have been performed of the $\Pi_{el}(h)$ and $\Pi_{VW}(h)$ as well as of their joint action at various electrolyte concentrations c. At very low c equilibrium films of large thickness formed

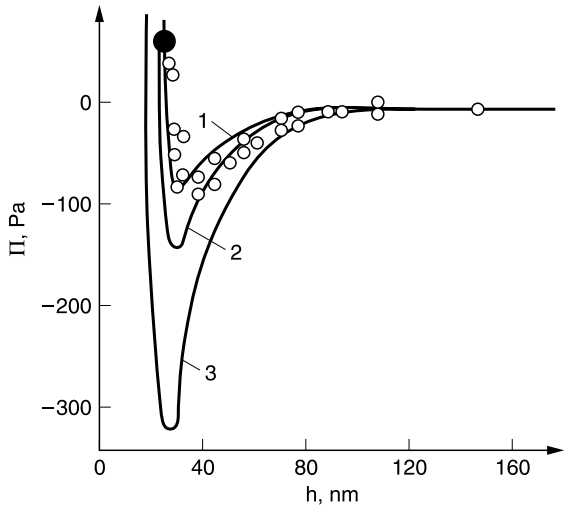

FIGURE 3.17 Disjoining pressure Π vs. film thickness h isotherm at 25 °C. Thin liquid film from 5×10^{-4} wt.% saponin + 0.01 M KCl aqueous solution. Solid lines: calculated according to Equations 3.73 and 3.74 with $\psi^0 = 90$ mV and $K_{VW} = 3.3 \times 10^{-21}$ J (curve 1), $K_{VW} = 5.1 \times 10^{-21}$ J (curve 2), $K_{VW} = 8.5 \times 10^{-21}$ J (curve 3); the point marked with • corresponds to the equilibrium film. (From A. Scheludko and D. Exerowa, *Kolloid-Z*, 165: 148 (1959); and 168: 24 (1960).)

in which the electrostatic interaction was prevailing and their behavior could be described completely with this interaction. At such film thickness Π_{VW} was still very low so that the equilibrium film state was reached at the balance of the electrostatic disjoining pressure and the capillary pressure, $\Pi_{el} = \Delta p_c$. Non-equilibrium thinning films were formed at high electrolyte concentration with prevailing action of the negative Π_{VW}. At intermediate electrolyte concentrations (10^{-2} to 10^{-3} mol dm^{-3}) Π_{el} and Π_{VW} are competitive. At large film thickness accelerated drainage was initially observed after which the process was delayed until equilibrium was established. This delay was due to the rise of Π_{el} with decreasing thickness. Figure 3.17 plots the $\Pi(h)$ isotherm obtained by the dynamic method for saponin aqueous films. The experimental point marked with full circle corresponds to an equilibrium film at $\Pi = \Delta p_c = 73$ Pa. In spite of the considerable data scattering an expressed minimum can be clearly seen, similar to the dependence calculated from Equations 3.69, 3.73, and 3.74 with $\psi^0 = 90$ mV and $n = 3$. The value of the van der Waals–Hamaker constant has been determined to be $K_{VW} = 4 \times 10^{-21}$ J, although one must keep note of the dependence of K_{VW} on the film thickness, predicted by Lifshitz' theory and calculated by some authors using approximate methods.

The DLVO surface forces have been studied [67] with equilibrium macroscopic vertical foam films from sodium octylsulfate aqueous solution containing KCl. The film thickness comprised a large range from 80 to 8 nm and electrolyte concentrations from 10^{-3} to 1 mol dm^{-3}. A smooth fall of the equilibrium thickness is clearly seen when the counter-ion concentration is increased. Studying films of small thickness, the authors considered for the first time film structure, i.e., the presence of an aqueous core and adsorption layers (Figure 3.2). This is important for the treatment of not only the results from optical thickness measurements but of $\Pi_{el}(h)$ and $\Pi_{VW}(h)$ as well. On the basis of these and other experimental data one can conclude that deviations from the DLVO theory appear at foam film thickness less than 20 nm.

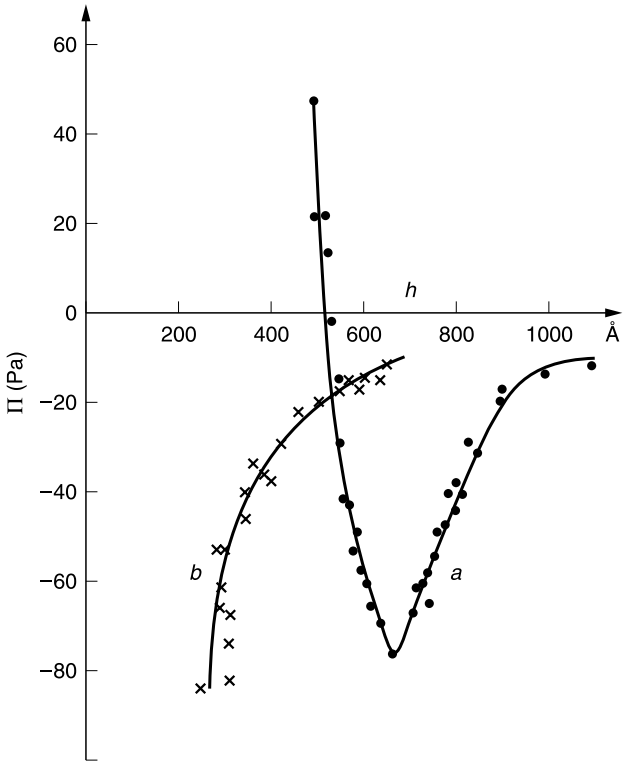

FIGURE 3.18 Disjoining pressure Π vs. film thickness h isotherm. Microscopic OWO emulsion films from NP20 aqueous solution between cyclohexane phases. Electrolyte concentration: 0.005 M KCl (curve *a*) and 2 M KCl (curve *b*). (From H. Sonntag, J. Netzel, and H. Klare, *Kolloid-Z Z Polym.* 211: 121 (1966).)

3.5.2.2 Experiments with Emulsion Films

Microscopic emulsion films have been studied [19] in the special measuring cell (Figure 3.5) using the microinterferometric technique. Both OWO and WOW films have been investigated. The dynamic method for assessment of the $\Pi(h)$ isotherms, based on Equation 3.11, has been used. Such experimental $\Pi(h)$ isotherms are presented in Figure 3.18 for emulsion films from aqueous solutions of NP20 (nonylphenylpolyethylenoxide20) + KCl in two different concentrations; the oil phase is cyclohexane. The right-hand curve *a* (with a minimum) has been obtained for an emulsion film from NP20 solution with 0.005 M KCl. At this low electrolyte concentration a significant Π_{el} arises with decreasing thickness after the minimum and the entire disjoining pressure $\Pi = \Pi_{el} + \Pi_{VW}$ becomes positive. At film thickness of 51.5 nm (Figure 3.18) $\Delta p = \Pi$ and an equilibrium film is established. The equilibrium film thickness h depends on the electrolyte concentration c, namely h decreases with increasing c.

Completely different $\Pi(h)$ dependence (Figure 3.18, left-hand curve *b*) has been obtained [19] for an emulsion film from the same NP20 solution, but with high electrolyte concentration $c = 2$ M KCl. The Π_{el} is now very low and can be neglected. The measured Π is practically Π_{VW} only; it is negative at all thicknesses and no equilibrium film can be obtained. The emulsion film wears thin until its rupture.

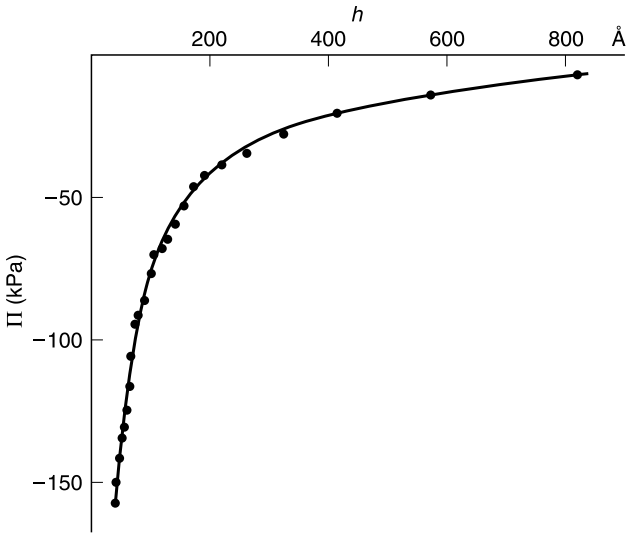

FIGURE 3.19 Disjoining pressure Π vs. film thickness h isotherm. Microscopic WOW emulsion films from 0.2 g dm^{-3} Span80 in octane solution between aqueous phases with electrolyte concentration 0.05 M KCl. (From H. Sonntag, J. Netzel, and H. Klare, *Kolloid-Z Z Polym.* 211: 121 (1966).)

The behavior of the WOW emulsion films from solutions of a nonpolar liquid ("oil") is similar. There are no ions dissolved in such a liquid, no double layers, and hence no Π_{el}. Figure 3.19 presents a $\Pi(h)$ isotherm obtained [19] for an emulsion film from Span80 solution in octane. The adjacent liquid phases are from 0.05 M KCl aqueous solution. Again the measured Π is Π_{VW} only, negative at all thicknesses, and the emulsion films always rupture since no equilibrium film can be obtained. All these results are in agreement with the DLVO theory.

3.5.2.3 Potential of the Diffuse Double Layer at the Film's Interface

Under certain conditions aqueous electrolyte solutions form equilibrium thin foam or OWO emulsion films. Their equilibrium thickness is determined by the positive electrostatic disjoining pressure Π_{el} which depends on the potential ψ^0 of the diffuse double layer at the liquid film/gas (or oil) interface. The relation between film thickness h and electrolyte concentration c obeys the DLVO theory of electrostatic disjoining pressure (Equations 3.70 and 3.71). The potential ψ^0 at the film's interface can be calculated from the measured equilibrium film thickness h and known c value. This is the "method of the equilibrium thin film" for determining the ψ^0-potential [68] and for studying the electric properties at the interface. The method provides a valuable possibility since an equilibrium potential and, respectively, surface charge density σ^o can be evaluated and all complications occurring at kinetic measurements are avoided.

Detailed study with the "method of equilibrium foam film" of the $h(c)$ and h(pH) dependence in the absence of a surfactant [68], as well as $h(c_s)$ at very low surfactant concentrations c_s, gave $\psi^0 \approx 30$ mV at the interface aqueous electrolyte solution/air. The ψ^0-potential at low electrolyte concentrations c increases with increasing c_s from its value for an aqueous electrolyte solution without surfactant to a constant value, typical for each surfactant kind [17]. The increase of ψ^0 at low concentrations c_s is connected with the surfactant's adsorption at the solution/air interface.

The surface charge density σ^o reaches a constant value when or just before the adsorption layer becomes saturated.

The values of the ψ^0-potential of the diffuse double layer at the surfactant aqueous solution interface can be used to calculate the surface charge density σ^o, according to

$$\sigma^o = [2\varepsilon RTc/\pi]^{1/2}\left[1/2\cos h\left(F\psi^0/RT\right) - 1/2\cos h\left(F\psi^m/RT\right)\right]^{1/2} \tag{3.79}$$

The calculation by the DLVO theory does not give an estimation whether the values of ψ^0 and σ^o are positive or negative. However, experimental measurements provide information which are the ions adsorbed at the interface and it is possible to determine the potential sign.

The ψ^0-potential (respectively σ^o) is considerably lower for nonionic surfactants but slightly higher than ψ^0 at the aqueous electrolyte solution/air interface, e.g., $\psi^0 = 39$ mV for decylmethylsulfoxide. For ionic surfactants such as Na dodecylsulfate, ψ^0 is essentially higher ($\psi^0 = 82$ mV). The ψ^0 values are in good agreement with the data for the ζ-potential obtained through electrophoresis of bubbles [70]. The very weak $\psi^0(h)$ dependence has indicated that the ψ^0 values can be accepted for the surface of the bulk liquid phase as well.

The ψ^0-potential at the aqueous electrolyte solution/air interface without surfactant has been measured very precisely at low electrolyte concentration and extremely pure solutions and vessels. The ψ^0(pH) dependence for aqueous solutions at constant ionic strength (HCl + KCl) shows that at pH > 5.5, the potential becomes constant and equal to about 30 mV. At pH < 5.5 the potential sharply decreases and becomes zero at pH $\approx$ 4.5, i.e., an isoelectric state at the solution surface is reached [68]. It is clear that the isoelectric state is controlled by the change in pH. This is very interesting, for it means that the charge at the surface of the aqueous solutions is mainly due to the adsorption of H^+ and OH^- ions. The estimation of the adsorption potential of these ions in the Stern layer showed that the adsorption potential of the OH^- ions is higher. It follows that the ψ^0-potential at a solution/air interface appears as a result of adsorption of OH^- ions [68].

3.5.3 Steric Surface Forces

The dispersion systems emulsion and foam contain practically always different surfactants as stabilizing agents. Hence for thin liquid films with fluid interfaces (emulsion or foam films) the most important *non-DLVO surface forces* are the *steric interactions*: short range for small molecules (to be discussed in the next section) and long range for macromolecules, which are considered here.

Microscopic foam films have been used to study the steric interaction between two liquid/gas interfaces [71]. Two ABA triblock copolymers have been employed: P85 ($PEO_{27}PPO_{39}PEO_{27}$, $M = 4600$ Da) and F108 ($PEO_{122}PPO_{56}PEO_{122}$, $M = 14000$ Da). Blocks A are hydrophilic polyethylene oxide (PEO) chains, while block B is a hydrophobic polypropylene oxide (PPO) chain. The film thickness has been measured by the micro-interferometric method. Figure 3.20 presents the dependence of the equivalent film thickness h_w on the electrolyte concentration c for aqueous solutions of the two copolymers. The h_w values initially decrease with increasing c and then level off at a constant value. The plateau starts at a *critical electrolyte concentration* $c_{cr} = 3 \times 10^{-3}$ mol dm^{-3} NaCl for F108 and $c_{cr} = 3 \times 10^{-2}$ mol dm^{-3} NaCl for P85, similar to the low molecular mass surfactants. The bulk properties of aqueous solutions of PEO–PPO–PEO copolymers are essentially similar to those of nonionic surfactants. It is very likely that the interaction behavior is determined by the hydrophilic PEO chains protruding into the solution.

The left branch of the $h_w(c)$ dependence (Figure 3.20) is dominated by electrostatic repulsion. The copolymers are nonionic and charge creation may be attributed to preferential adsorption of

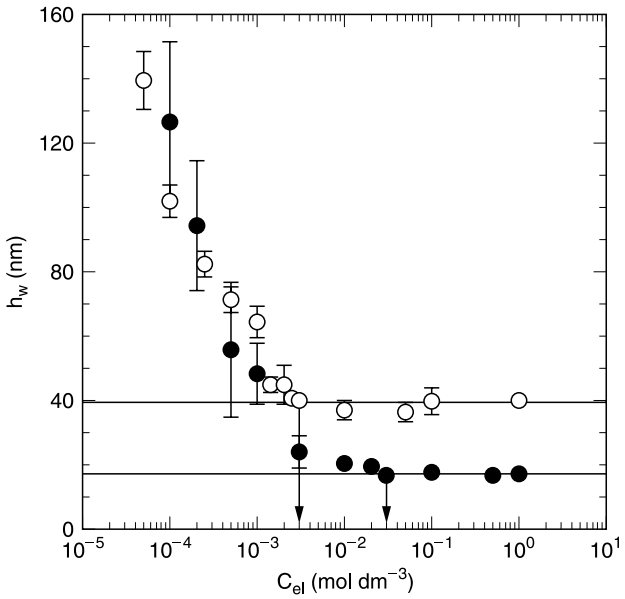

FIGURE 3.20 Equivalent film thickness h_w vs. NaCl concentration c_{el} at 23 °C. (●): 7×10^{-5} M P85 aqueous solutions; (○): 7×10^{-7} M F108 aqueous solutions. The arrows show the corresponding c_{cr}. (From D. Exerowa, R. Sedev, R. Ivanova, T. Kolarov, and ThF. Tadros, *Colloids Surfaces* 123; 277 (1997).)

OH^- ions at the air/water interface. The data for both copolymers located below their c_{cr} roughly follow the same trend (Figure 3.20). On the contrary, the plateau values for the two copolymers are very different: 39 ± 3 nm and 17 ± 1 nm, respectively. Since the higher copolymer gives thicker films a surface force component of steric origin may be evoked. However, the thickness h_w is an effective parameter which is too crude. As a reasonable compromise between physical relevance and tractability, the three-layer model is adopted (Figure 3.2). The equivalent film thickness h_w is larger than the total film thickness h, since the refractive index of the adsorption layer is higher than that of water ($n_1 > n_2$). Allegedly, the electrolyte concentration affects only the aqueous core thickness h_2 which can be calculated using Equation 3.4.

The thickness h_1 of the adsorption layer is determined by the conformation of the macromolecules at the interface. The radius of gyration R_F of a flexible neutral chain in good solvent is given [72] by the Flory relation:

$$R_F = aN^{3/5} \tag{3.80}$$

where a (~0.2 nm) is an effective monomer size and the number $N = N_{PO} + 2N_{EO}$. If a macromolecule adsorbs at the interface as a separate coil, it should occupy an area of the order of the projected area of the molecule in the bulk solution, i.e., R_F^2. The figures obtained (~2 nm^2) are much lower and, therefore, the PEO chains are crowding the solution/air interface and stretched, i.e., they form a brush [73]. Its thickness h_1 can be calculated from the simple brush model:

$$h_1 = aN_{EO}\left(a^2/A_o\right)^{1/3} \tag{3.81}$$

A_o being the area per molecule.

The most significant finding is that the plateau thickness values at high electrolyte concentration are larger than twice the adsorption layer thickness: $h > 2h_1$. This is rather unexpected since above c_{cr}, electrostatic repulsion is suppressed and steric interaction alone is expected to stabilize the film. If so, a total thickness close to the double brush thickness, i.e., $h \approx 2h_1$, would be expected. Both h and h_1 are different for the two copolymers. However, the thinnest films from both copolymers have the same structure: two brush layers and an aqueous core of thickness $\sim 3R_F$. The equilibrium thickness of the thinnest films is probably due to the same type of steric stabilization which is different from the brush-to-brush repulsion.

Quite similar results have been reported [74] for foam films from aqueous solutions of polyvinyl alcohol. Their equilibrium thickness at low pressure is much larger than twice the adsorption layer thickness measured by ellipsometry. The core thickness is again several times the radius of gyration of the polymer molecules in bulk solution. The explanation given in Ref. 74 is that the upper limit of interaction is governed by few, essentially isolated, polymer tails. Similar arguments can also be given in the case of an ABA block copolymer. In other words the film thickness at high electrolyte concentration is governed by the longest, and not the average, PEO chains. A chain longer than the average brush thickness will behave as a brush only up to h_1, but as a mushroom (swollen coil) further into the solution.

Thus, the following qualitative picture is arrived at: above c_{cr}, at lower pressure the mushroom tails of the longer chains interact rather softly; at higher pressure a brush-to-brush contact is realized and steeper repulsion is expected. This behavior is experimentally confirmed. At lower c electrostatic repulsion dominates and decreases until steric repulsion (which is independent of c) becomes operative at c_{cr}. The transition from electrostatic to steric repulsion occurs at c_{cr} given by

$$\frac{1}{\kappa_{cr}} \equiv \left(\frac{\varepsilon \ kT}{8\pi \ e^2 N_A c_{cr}} \right)^{1/2} = R_F \tag{3.82}$$

where ε is the dielectric constant of the medium; e is the elementary charge; N_A is Avogadro's number; $1/\kappa_{cr}$ is the Debye length at c_{cr}.

The most detailed information about the steric surface forces can be obtained [75] from the disjoining pressure vs. thickness isotherm $\Pi(h)$ for films from polymer aqueous solutions with $c > c_{cr}$. The two cases discussed above can be clearly distinguished: (1) at low pressures, $\Pi < 10^2$ Pa, the "soft" steric repulsion determines quite large film thickness of about 40 to 50 nm; (2) at high pressures, $\Pi > 10^2$ Pa, a strong steric repulsion due to the brush-to-brush contact determines considerably smaller thickness. Presumably, the PEO brushes extending from the two surfaces come into contact and repel each other. Under these conditions the de Gennes scaling theory [73] for interaction between two surfaces carrying polymer brushes applies. Accordingly the steric disjoining pressure is given by

$$\Pi_{st} \cong \frac{kT}{D^3} \left(H^{-9/4} - H^{3/4} \right) \tag{3.83}$$

where $H = h/2h_1$ is the dimensionless film thickness (h_1 is the brush layer thickness at infinite separation); D is distance between two grafted sites. The first term is osmotic pressure arising from the increased polymer concentration in the two compressed layers. The second one is an elastic restoring force (polymer molecules always tend to coil and hence the negative sign of this term). De Gennes' theory gives a satisfactory description of the steric surface forces at pressures and film thickness where brush-to-brush contact is realized.

3.5.4 Oscillatory Disjoining Pressure

A consecutive stepwise film thinning has been observed at thin liquid films with fluid interfaces, formed from solutions with surfactant concentration much higher than CMC. This is the phenomenon known as *stratification*. During this process the initially formed films thin to smaller and smaller thickness, reaching black films in most of the cases, sometimes even down to bilayers. The stratification phenomenon in foam films has been described at the beginning of the twentieth century [5,76]. Later the stepwise thinning was studied by many authors [77–81] and it became evident that this phenomenon is universal and, in addition to being observed in emulsion and foam films, it has also been seen in asymmetric films of the air/water/oil type, films from latex suspensions, liquid crystalline films, etc.

The stratification phenomenon is connected with the layered ordering of molecules or micelles inside the film. During drainage these ordered layers of molecules or micelles flow out towards the film's periphery (the meniscus that surrounds the film), i.e., the film thinning occurs stepwise, layer after layer. It has been pointed out that this phenomenon is caused by oscillation in the Gibbs free energy of the film when its thickness is changed. Two theories have emerged to account for these Gibbs energy oscillations: bilayers of amphiphile molecules in the film structure or cubic lattice of ordered micelles. The "combined" structuring of films is also possible.

Very precise measurements of $\Pi(h)$ isotherms have been performed [22] with foam films from aqueous high concentrated solutions of Na dodecylsulfate, employing both the pressure balance technique and the dynamic method. The disjoining pressure isotherms were established down to pressures of 10 Pa with specially constructed film holders and careful pressure isolation and control. The typical $h(t)$ curve shows a film thinning with a step of 10 nm. The stepwise thinning has been explained by the oscillatory form of the $\Pi(h)$ isotherm (Figure 3.21). At constant capillary pressure an oscillating driving force develops that produces the observed stepwise thinning.

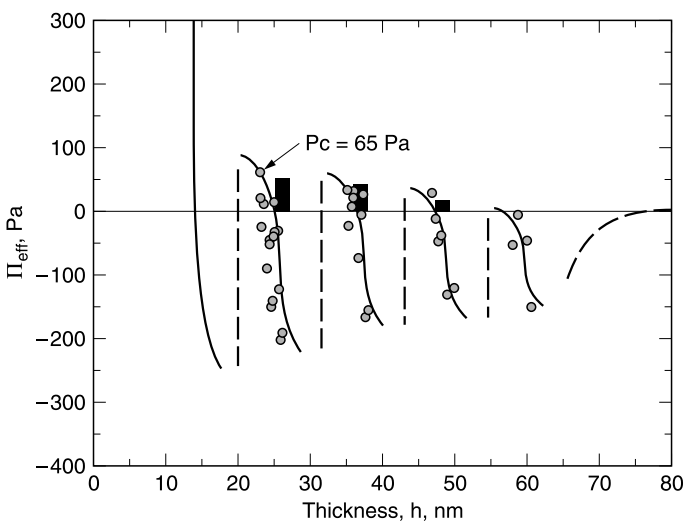

FIGURE 3.21 Oscillatory disjoining pressure Π vs. film thickness h isotherm at 24 °C. Thin liquid films from 0.1 M Na dodecylsulfate aged aqueous solution. (○): dynamic method; (■): equilibrium films. (From V. Bergeron and C.J. Radke, *Langmuir* 8: 3020 (1992).)

The authors introduced the term *oscillatory disjoining pressure* [22]. As seen from Figure 3.21, the results obtained by the dynamic and the equilibrium methods conform well. The former gives also negative values of disjoining pressure which is an advantage of this method. It is worth noting that the length scale of the oscillations was large, about 10 nm, and even reached about 50 nm. A theoretical analysis was based on the equilibrium "oscillatory structural component" of disjoining pressure. It is clear that the oscillatory disjoining pressure is due to structures of surfactant molecules, including micelles, in the thin liquid film. However, it is commonly accepted that the structural component of disjoining pressure is determined by the structuring of solvent molecules. Hence the question if the oscillatory disjoining pressure could be considered as a kind of structural disjoining pressure is open.

3.6 BLACK EMULSION AND FOAM FILMS

3.6.1 Two Equilibrium Phase States of Black Films

During their thinning, thin liquid films lose their stability at a certain critical thickness h_{cr}. Depending on the type of surfactant and its concentration a jump-like formation of *black spots* in the emulsion or foam films can occur. The black spots expand, merge, and at the end the entire film area is occupied by *black film* (Figure 3.14). These films can reach extremely small thicknesses. Observed under a microscope they reflect very little light and appear black when their thickness is below 20 nm. Therefore, they could be called nanofilms as well. The IUPAC nomenclature [82] distinguishes two equilibrium phase states of black films: *common black film* (CBF) and *Newton black film* (NBF). There is a pronounced transition between them, i.e., CBF can transform into NBF or the reverse [83].

The CBF, just as the common thin liquid films, can be described by the three layer film model or "sandwich model," a liquid core between two adsorption layers of surfactant molecules (Figure 3.2). The NBF, however, are bilayer formations without a free liquid core between the two layers of surfactant molecules [83]. Thus, the contact between droplets, respectively bubbles, in the emulsion or foam can be achieved by bilayer from amphiphile molecules. In the behavior of the latter the short-range molecular interactions prove to be of major importance. The definition "liquid film" is hardly valid for bilayers. They possess a higher degree of ordering similar to that of liquid crystals.

The disjoining pressure vs. thickness dependence for relatively large h values of common thin liquid films, stabilized by surfactants, is consistent with the DLVO theory. However, black films exhibit a diversion from the DLVO theory which is expressed in the specific course of the $\Pi(h)$ isotherm. Figure 3.22 depicts a $\Pi(h)$ isotherm (in arbitrary scale) of an aqueous emulsion or foam film from a surfactant solution containing an electrolyte. The two states of black films, CBF and NBF, are clearly distinguished. Such a presentation of the $\Pi(h)$ isotherm can explain the thermodynamic phase state of the two types of black films stabilized by long- and short-range surface forces, respectively.

In the right-hand side of the isotherm (Figure 3.22) the curve passes a shallow minimum, after which the disjoining pressure becomes positive and increases up to a maximum. In this range common thin liquid films exist, their equilibrium being described by the DLVO theory. If $h < h_{cr}$, the film is a common black film, CBF, schematically presented in the figure. Such a film forms via black spots and at the equilibrium film thickness h_1 the disjoining pressure equals the external (capillary) pressure, $\Pi = \Delta p$. The equilibrium of CBF is also described by the DLVO theory, although discrepancies between the theoretical and experimentally obtained

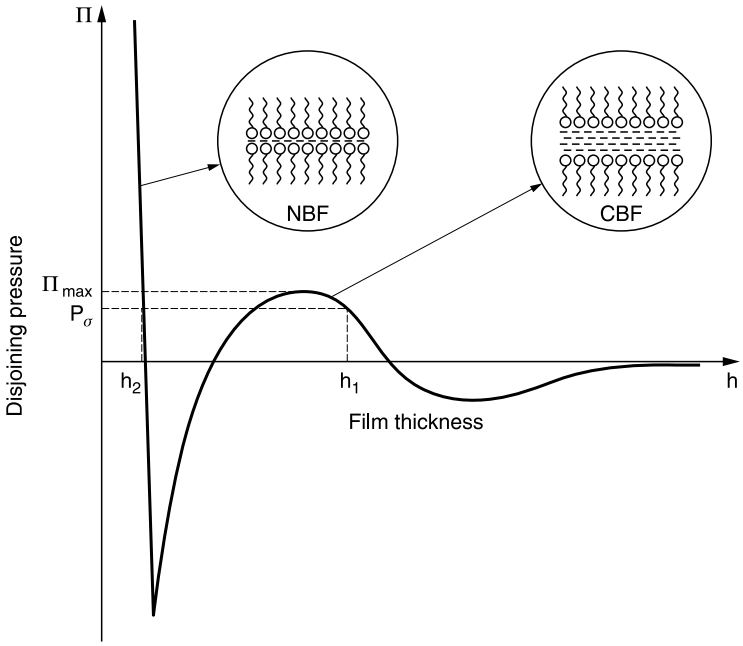

FIGURE 3.22 Schematic presentation of a disjoining pressure Π vs. film thickness h isotherm of a symmetric thin liquid film in arbitrary scale.

$\Pi(h)$ isotherms at film thickness below 20 nm are established [83,84]. The pressure difference $\Pi_{\max} - \Delta p$ is the barrier which hinders the transition to a film of smaller thickness.

According to the DLVO theory, after $\Pi_{\max}$ the disjoining pressure should decrease infinitely in direction of thickness decrease. However, the experimental results [24,85] show the existence of a second minimum in the $\Pi(h)$ isotherm after which the disjoining pressure sharply ascends. Another equilibrium is established on the rising left hand side of the isotherm, again under the condition $\Pi = \Delta p$. This black film with a smaller equilibrium thickness h_2 is actually the bilayer Newton black film (NBF), schematically presented in the figure as well. The left branch of the $\Pi(h)$ curve, like the preceding minimum, is not described by the DLVO theory. Obviously at this extremely small film thickness short range non-DLVO surface forces, for instance steric interactions, determine this part of the $\Pi(h)$ isotherm.

3.6.2 Disjoining Pressure in Black Films

The direct experimental measurement of the disjoining pressure Π and the film thickness h (the $\Pi(h)$ isotherm) is of major importance for understanding the nature of surface forces which determine the equilibrium state of both types of black film as well as to establish the CBF/NBF transition. It turned out that the Thin Liquid Film–Pressure Balance Technique (Figure 3.7), employing the porous plate measuring cell of Exerowa–Scheludko (Figure 3.3, B), provides the equilibrium values in a wide range of pressures and thicknesses. This technique has been successfully applied by many authors for plotting $\Pi(h)$ isotherms of black films from various surfactant solutions. The different kinds of surfactants (emulsion or foam stabilizers) show some peculiarities in the $\Pi(h)$ isotherms.

3.6.2.1 Ionic Surfactants

Black films from Na dodecylsulfate (NaDoS) will be considered here as an example for plotting $\Pi(h)$ isotherms, since films from this typical representative of ionic surfactants and very good stabilizer of emulsions and foams have been studied extensively [21,22,86] and most of the film parameters are well known. Figure 3.23 presents the experimental results obtained by three different teams at different times. The figure indicates a good agreement between the data of all authors in the right-hand side of the curve, i.e., for the long-range interactions. However, Mysels and Jones did not present data for the left-hand side of the isotherms, i.e., within the NBF region and the CBF/NBF transition, since the porous ring measuring cell they employed does not allow such measurements; Bergeron and Radke used the porous plate measuring cell.

If Figure 3.23 is compared with the $\Pi(h)$ isotherm drawn in arbitrary scale in Figure 3.22, it can be seen that positive Π values only have been measured, since equilibrium black films form only when the positive $\Pi = \Delta p$. It is clear that when $(d\Pi/dh) > 0$, films are thermodynamically unstable and their thickness cannot be measured. The right branch of the $\Pi(h)$ curve refers to CBF and indicates that their thickness h decreases with increase in Δp. When a thickness of 7.1 nm is reached at $\Pi_{max} \approx 10^5$ Pa, the CBF transforms through a jump-like transition into NBF of $h = 4.3 \pm 0.2$ nm. The increase in capillary pressure up to 1.2×10^5 Pa does not alter the NBF thickness. NBF does not change its thickness also with the decrease in pressure down to $\Delta p = 0.1 \times 10^5$ Pa. Around this point, however, again with a jump, it transforms into a CBF with the corresponding thickness [21].

In the electrolyte concentration range $c = 0.165$ to 0.18 mol dm^{-3} a pressure region of fluctuating NBF/CBF transition has been found [21]. At higher electrolyte concentrations when a certain pressure value is reached, a jump-like transition CBF to NBF occurs. The film thickness of such a transition does not depend on c which means that there is a fluctuation zone where the energy needed to overcome the barrier Π_{max} in the $\Pi(h)$ isotherm (Figure 3.22) is of the order of kT. Films that satisfy this energy requirement are called metastable films. Upon increasing c the pressure, at which the transition occurs, reduces as a result from lowering of the barrier Π_{max}.

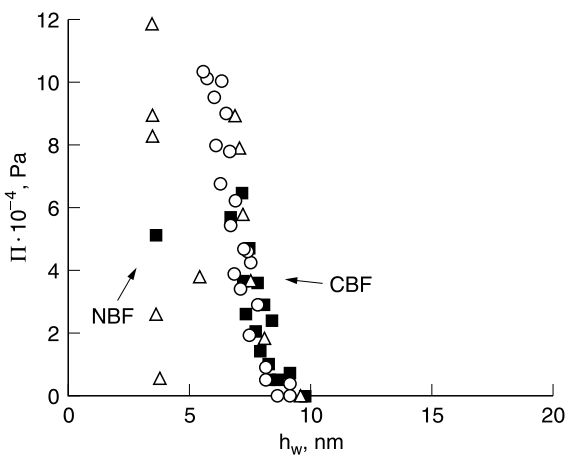

FIGURE 3.23 Disjoining pressure Π vs. film thickness h_w isotherms at 23 to 24 °C. Thin liquid films from 1 mM Na dodecylsulfate + 0.18 M NaCl aqueous solution. (△): data from Ref. 21; (■): data from Ref. 22; (○): data from Ref. 86.

At $c > 0.2$ mol dm^{-3} there is no NBF to CBF transition occurring, which means that the left minimum in the $\Pi(h)$ isotherm lies deeply into the region of negative Π values. Thus, an electrolyte concentration range from 0.165 to 2.0 mol dm^{-3} confines the isotherm region in which both CBF/NBF and NBF/CBF transitions can take place. The NBF thickness measured (within the experimental accuracy) does not depend on capillary pressure and its average value is 4.3 nm. This value will be further discussed again. Similar $\Pi(h)$ isotherms have been depicted also for other anionic surfactants [87].

3.6.2.2 Nonionic Surfactants

Two type $\Pi(h)$ isotherms have been established [88] for black films from aqueous solutions of nonionic surfactants. The first one can be illustrated by solutions of $C_{10}(EO)_4$ (decyl 4-oxyethyl), the surfactant and electrolyte concentrations being chosen so that equilibrium films within a large thickness range are obtained, including the CBF/NBF transition region. The change in film thickness has been achieved by gradually and isothermally increasing the capillary pressure. The initial thickness of the $C_{10}(EO)_4$ film decreases down to 11 nm and black spots appear, gradually invading the whole film and turning it black. Its thickness falls to 6 nm and does not change upon further increase in capillary pressure. This result indicates that the transition to NBF occurs via a jump-like transition overcoming the $(\Pi_{max} - \Delta p)$ barrier, i.e., the $\Pi(h)$ isotherm has the same shape as that in Figure 3.23.

The other type $\Pi(h)$ isotherm can be illustrated by black films of NP20 (20-oxyethyl nonylphenol). The experimentally obtained curve follows another course. With the increase in Π the film thickness decreases gradually without any jump-like transition and an equilibrium thickness of 9 nm is reached. It remains constant with further increasing of the pressure. Since the ψ^0-potential is almost equal for both surfactants, there should be an additional repulsion force in the NP20 films. Knowing that the thickness of these films does not depend on c but is a function of Π such an assumption seems reasonable. That is why it is interesting to see whether the experimental isotherms conform with those derived from the DLVO theory.

The experimental $\Pi(h)$ curve for films from $C_{10}(EO)_4$ lies between the two theoretical curves obtained at $\sigma^o = \text{const}$ and $\psi^0 = \text{const}$. Therefore, it can be supposed that in this case the DLVO theory describes well the electrostatic and van der Waals interactions in the common black films. The experimental $\Pi(h)$ isotherms of NP20 films are in agreement with the theory only in the right-hand side of the isotherm, at relatively large thickness. The curve follows a smooth course which probably reflects the existence of gradually increasing force additional to Π_{el} repulsive force. As far as this force appears in films from surfactants with long oxyethylene chains, it can be considered as steric interaction.

The $\Pi(h)$ isotherms of black films from NP20 solutions measured at pH = 5.7, 6.1, and 4.0 have clearly shown the influence of OH^- ions [88] and the isotherms are in a very good agreement with the h(pH) dependence determined at $\Delta p = \text{const}$. Detailed quantitative analysis (using the nonlinear Poisson–Boltzmann equation) of the disjoining pressure experimental values obtained with black films from nonionic sugar-based surfactant [89] at various c_s, pH, and ionic strength have also shown that the OH^- ions create the surface charge at the film/air interface.

3.6.2.3 Phospholipids

Formation of thin aqueous films from phospholipids is a difficult task since many of them are insoluble in water. Sonicated dispersions of insoluble phospholipids is an option [90], and direct measurement of interaction forces in films stabilized by neutral phospholipids was first done

with films from suspensions of unilamellar DMPC vesicles [91]. The $\Pi(h)$ isotherm indicates a barrier transition to NBF and Newton black spots appear in the CBF. The NBF thickness of 7.6 nm remains constant with further increase in pressure. This isotherm is similar to the one obtained for nonionic surfactants such as $C_{10}(EO)_4$. The right-hand side of the isotherm can be interpreted in the same way with DLVO surface forces.

Interesting results have been obtained for black films stabilized by soluble zwitterionic phospholipids [92]: lysophosphatidylcholine (lyso PC) and lysophosphatidyl ethanolamine (lyso PE) in the presence of Na^+ and Ca^{2+}. Besides the $\Pi(h)$ isotherm, another type of isotherm proves to be very informative, namely the dependence of film thickness h on electrolyte concentration c, at $c_s = \text{const}$, $\Delta p = \text{const}$, and $T = \text{const}$. This $h(c)$ dependence allows the action of electrostatic disjoining pressure to be distinguished clearly and the electrolyte concentration at which the CBF/NBF transition occurs to be found.

The effect of Ca^{2+} on the equilibrium thickness of films from lyso PC aqueous solution [93] is shown in Figure 3.24. Unlike the results obtained with the monovalent Na^+ ions, black films of constant thickness $h = 7.6$ nm have always been formed at low Ca^{2+} concentrations. At 0.001 mol dm^{-3} $CaCl_2$, however, a dramatic increase in film thickness to about 35 nm has been observed, i.e., a transition to relatively thick films occurred. Further increase in c leads to a monotonous decrease in film thickness until c reached 0.02 mol dm^{-3} $CaCl_2$ where gradually expanding black spots appeared, until the whole film became black. The thickness of these black films (obviously CBF) continues to decrease with increase in c up to 0.2 mol dm^{-3} $CaCl_2$ when again black films of the same thickness as that in the low concentration range are obtained. This is indicated in Figure 3.24 by a small thickness jump. Further increase in c up to 0.5 mol dm^{-3} has no effect on the thickness of these black films. The $\Pi(h)$ isotherm at 0.002 mol dm^{-3} $CaCl_2$ is also similar to that for $C_{10}(EO)_4$: relatively thick films are formed at low pressures and their

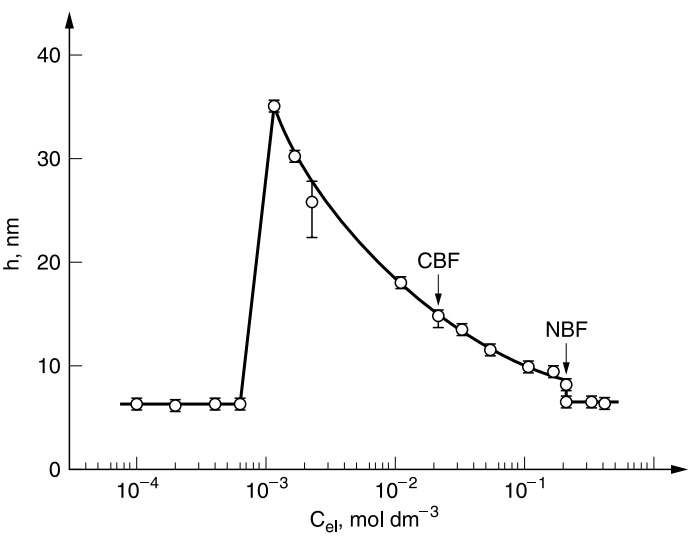

FIGURE 3.24 Equivalent film thickness h vs. $CaCl_2$ concentration c_{el} at 30 °C. Microscopic foam films from lyso-phosphatidylcholine aqueous solution, pH = 5.5, $\Delta p = 35$ Pa. (From R. Cohen, D. Exerowa, T. Kolarov, T. Yamanaka, and V.M. Muller, *Colloids Surfaces* 65: 201 (1992).)

thickness decreases with increase in Π. After a jump-like CBF/NBF transition the NBF thickness does not change with further increase in pressure.

Measurements involving different techniques have shown that monovalent ions practically do not bind to zwitterionic phospholipids. In contrast, the observed thickness transition in Figure 3.24 clearly demonstrates that the divalent Ca^{2+} ions have a specific effect on the properties of the black films studied. Most probably this is due to the specific binding of Ca^{2+} ions to the adsorbed lyso PC [94]. The binding of the positive Ca^{2+} ions in the low concentration range can lead to low ψ^0-potentials, consequently, to a decrease in the electrostatic repulsion, and to formation of NBF. The transition from NBF to thicker films can be related to further Ca^{2+} ion binding at higher c that induces higher ψ^0 values. The corresponding Π_{el} is evidently sufficient to allow for the formation of thicker films. Further increase in c leads to film thickness diminishing as a result of the competitive action of further Ca^{2+} binding (higher ψ^0-potential) and higher ionic strength of the solution (lower Π_{el}).

3.6.3 Properties of CBF and NBF and the Transition between Them

The two types of black film, common black film (CBF) and Newton black film (NBF), seem to be similar: obtained from the same surfactant solution, both are very thin ($h < 20$ nm). However, they show rather different properties due to their different structure and they are two different equilibrium phase states of a black emulsion or foam film [83]. This difference determines the CBF/NBF transition as well. A number of thermodynamic parameters determine if CBF or NBF is in equilibrium: temperature T, electrolyte concentration c, surfactant concentration c_s, pH, and capillary pressure Δp. Besides the values of these parameters, the kind of the surfactant (including amphiphile polymers) is also decisive for the existence of the black films. The parameter values, at which a CBF or an NBF is stable, are in definite (sometimes narrow) intervals and only the combination of all parameters determines a given type of black film.

The following example illustrates this. The good emulsion or foam stabilizer NaDoS (Na dodecylsulfate) provides formation of stable black films only if its concentration $c_s > c_{bl}$ (c_{bl} is the concentration of black spot formation; see Section 3.3.4). However, the c and $\Delta p = \Pi$ values are also decisive. They determine if the films either rupture or a CBF/NBF transition occurs at a given film thickness h. In the NaCl concentration range 10^{-4} to 0.15 mol dm^{-3}, the films rupture in a certain pressure interval which becomes narrower with the rise in c.

The temperature is another very important parameter: systematic studies [95,96] of black foam films from NaDoS aqueous solutions have shown that at given c, c_s, and Δp the change of temperature causes CBF/NBF transition; at high temperatures the equilibrium black films are CBF and at low temperatures, NBF. In Figure 3.25 the line splits up the diagram between the area of CBF stability (left and upper part) and the area of NBF stability (right and lower part).

The influence of temperature is well demonstrated by measurements [97] of the longitudinal specific electrical conductivity κ_f of black foam films from NaDoS solution. The temperature dependence of κ_f of CBF in Arrhenius coordinates has the same slope as the temperature dependence of the specific electrical conductivity κ of the bulk solution. The slope of the line for NBF is much steeper. The cross-point of both lines at 31.6 °C indicates the temperature of the CBF/NBF transition at the given concentrations of the initial solution. The slope of these lines in Arrhenius coordinates is proportional to the activation energy of the ions' movement. The almost equal slopes of the lines for CBF and bulk solution indicate that the liquid core of CBF contains practically the same solution as in the bulk. On the contrary the 2.5 times larger slope of the line for NBF proves that the NBF does not contain any liquid solution.

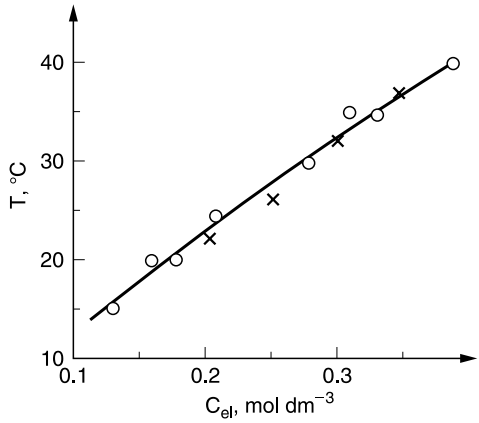

FIGURE 3.25 Temperature T of the CBF/NBF transition vs. electrolyte concentration c_{el}. Black films from Na dodecylsulfate aqueous solutions. (×): data from Ref. 95; (○): data from Ref. 96.

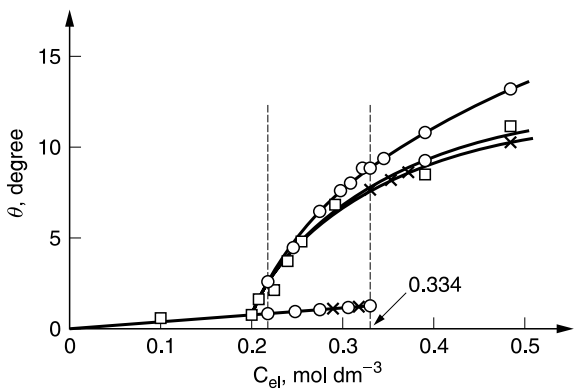

FIGURE 3.26 Contact angle θ vs. NaCl concentration c_{el} at 22 °C. Black films from Na dodecylsulfate aqueous solutions. (×): data from Ref. 24; (□): data from Ref. 85; (○): data from Ref. 98.

Another very informative fact is that the transport numbers of the counter-ions in NBF from ionic surfactants are close to 1, i.e., the electric current is due to the surfactant counter-ions only; the film contains practically no other ions although high electrolyte concentration is present in the bulk solution. The transport numbers of ions in CBF are almost the same as in the bulk.

Thermodynamic quantities which show rather different values for CBF and NBF are the contact angle α_o and film tension γ^f related through Equation 3.64. Systematic measurements of α_o have been performed with black foam films from NaDoS aqueous solutions [24,85,98]. Figure 3.26 presents the results obtained by three different teams. A very sharp jump in the $\alpha_o(c)$ curve is observed at the CBF/NBF transition. The critical electrolyte concentration c_{cr} at which the transition occurs from one type of black film to the other can be determined from this jump. For instance, for microscopic black films from NaDoS + NaCl solutions, $c_{cr} = 0.334$ mol dm^{-3}. At lower c values, CBF with $\alpha_o < 1°$ are stable while at higher c values, NBF with α_o of the order

of 10° are stable. The data obtained for macroscopic flat films in a frame indicate a bit lower values, i.e., $c_{cr} = 0.2$ mol dm^{-3}.

Hence, a range of NaCl concentration (0.2 to 0.334 mol dm^{-3}) is distinguished in which the $\alpha_o(c)$ curves follow a different course. This is due to the metastable state of CBF; in this concentration range the microscopic CBF transform into NBF after a certain time. In the metastable region, indicated by the dashed lines in Figure 3.26, both NBF and CBF are observed; respectively, large or small values of the contact angles. The α_o values obtained with microscopic NBF are close to those obtained with macroscopic NBF. When there is no external influence, NBF is only formed at electrolyte concentrations at which the maximum in the $\Pi(h)$ isotherm is overcome: $\Pi_{max} \leq \Delta p$. However, if the film area is large or the film is subjected to an external disturbance, NBF can be obtained at lower c when $\Pi_{max} > \Delta p$.

The film tension γ^f being related through Equation 3.64 with the contact angle α_o show similar behavior. Its value for CBF ($\alpha_o < 1°$) is close to 2γ of the bulk solution, while for NBF (α_o of the order of 10°) it is essentially different. Accordingly, the values of the interaction Helmholtz energy $\Delta F(h)$ of the film are rather different for CBF and NBF.

A completely different behavior exhibit the two types of black films from NaDoS solutions in another aspect. Contrary to CBF, the NBF do not change their thickness with Δp and c alterations. However, their properties depend on the composition of the bulk surfactant solution, e.g., α_o depends on c. The thickness of NBF determined from $h(c)$ dependence is approximately equal to the doubled thickness of the adsorption layer as assumed by Perrin. This is confirmed by NBF obtained from other surfactants. It has been proved, however, by infrared spectroscopy [99] and electrical conductivity measurements [97], that there is water in the NBF. It is most probable that the adsorption layers contain a certain quantity of water but they are not separated by an aqueous core. This is confirmed also by ellipsometric measurements [100].

The data for the film thickness of NBF from NaDoS solutions obtained by several authors with different techniques are rather scattered between 33 and 45 Å. Precise X-ray reflectivity measurements with CBF and NBF films from NaDoS + NaCl aqueous solutions provide more details about their structure [101]. The thickness of the respective layers which detail the film structure is: hydrocarbon chains layer 10.8 Å, polar groups layer 3.75 Å, water layer 3.75 Å, total film thickness 32.9 Å. Although these data indicate an aqueous core, this water is most probably not a liquid but hydration water and the NBF can be considered as bilayers.

3.6.4 Stability and Rupture of Bilayer Black Films

The Newton black foam films, the Newton black emulsion films, and the bilayer lipid membranes (BLM) are bilayers of amphiphile molecules. Their stability in respect to rupture and their permeability can be considered from a unified point of view [102,103]. Figure 3.27 represents schematically the generally accepted molecular model of such bilayers. The description of the fluctuation formation of microscopically small holes responsible for the bilayer stability and permeability can be based on both thermodynamic and molecular models.

The driving force or supersaturation $\Delta\mu$ for bilayer rupture is a thermodynamic quantity, since it is defined by

$$\Delta\mu = \mu_b - \mu_s \tag{3.84}$$

where μ_b and μ_s are, respectively, the chemical potentials of the amphiphile molecules in the bilayer and in the solution. For sufficiently dilute solutions μ_s is known to depend logarithmically on the concentration c_s of the monomer amphiphile molecules in the solution. Equation 3.84 can

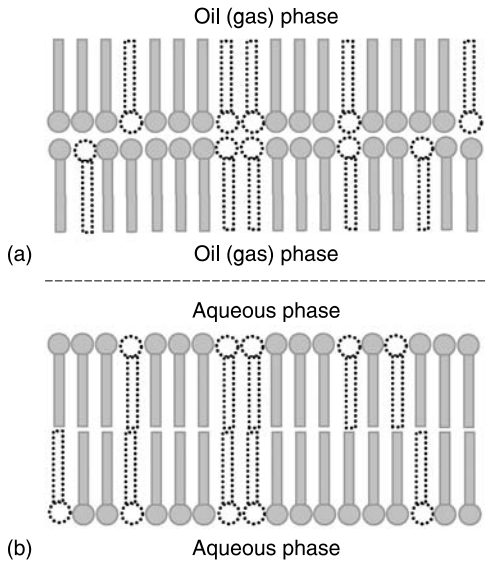

FIGURE 3.27 (a) Molecular model of OWO emulsion or foam bilayer film; (b) molecular model of WOW emulsion bilayer film or bilayer lipid membrane (BLM). The filled symbols denote amphiphile molecules; the dotted symbols schematize vacancies and holes.

be approximated by

$$\Delta\mu(c_s) = kT \ln\left(c_e/c_s\right) \tag{3.85}$$

where c_e is a certain concentration of monomer amphiphile molecules in the solution, called bilayer equilibrium concentration.

Thermodynamics can also be used for determining of the work w_i for fluctuation formation of an i-sized hole, $i = 1,2,3,\ldots$ being the number of amphiphile molecules that would fill the hole. Since the hole appears as a result of the passage of i molecules from the bilayer into the solution, the work associated with this process is $-i\Delta\mu$. On the other hand, work equal to the hole total peripheral free energy $P_i > 0$ is done in creating the hole periphery. P_i is proportional to the length of the hole periphery, which for circular holes of bilayer depth is $(2\pi A_0 i)^{1/2}$. Hence, w_i is given by

$$w_i = -i\Delta\mu + \tau_L (2\pi A_0 i)^{1/2} \tag{3.86}$$

where τ_L (J m^{-1}) is the hole specific edge free energy which, in principle, can be a function of i; A_0 is the area per molecule.

When $\Delta\mu > 0$ (for example, when $c_s < c_e$), the competition between the two energy terms in Equation 3.86 causes w_i to pass through a maximum of value. The hole of size i^* is the so-called nucleus hole, and w^* is the nucleation work. While the subnucleus holes tend to decay (w_i decreases with decreasing $i < i^*$), the supernucleus holes can grow spontaneously (w_i decreases with increasing $i > i^*$). For this reason, the bilayer can rupture only after the fluctuation appearance of at least one nucleus hole per unit time and, accordingly, w^* is the energy barrier

for bilayer rupture. If $\Delta\mu = 0$, i.e., if $c_s = c_e$, the bilayer is truly stable (and not metastable) in respect to rupture by hole nucleation. It must be emphasized that the bilayer also retains this true (or infinite) stability for $\Delta\mu < 0$, i.e., for $c_s > c_e$, since both terms in Equation 3.86 are then positive and w_i can only increase with increasing i. The bilayer cannot rupture despite the presence of a certain population of holes in it.

Let us turn to results obtained on the basis of the molecular model of amphiphile bilayer illustrated in Figure 3.27. The basic idea in the theoretical description is to regard the bilayer as consisting of two monolayers of amphiphile molecules mutually adsorbed on each other. Each of the monolayers can be filled with a maximum of $N_m = 1/A_0 \sim 10^{18}$ molecules m^{-2}, but the thermal motion of the molecules reduces their density below N_m. This means that vacancies of amphiphile molecules (i.e., molecule-free sites) exist in the bilayer, their density being n_1 (m^{-2}). At high values of n_1 the vacancies cluster together to form holes. If these holes are sufficient in number and size, they can make the bilayer permeable to molecular species. When $\Delta\mu > 0$, i.e., $c_s < c_e$, nucleus hole can come into being and, by irreversible overgrowth, cause the rupture of the bilayer. In other words, rupture occurs as a result of a two-dimensional first-order phase transition of the "gas" of amphiphile vacancies in the bilayer into a "condensed phase" of such vacancies which is equivalent to a ruptured bilayer.

The lattice model of the bilayer (Figure 3.27) can also be used to express c_e in terms of intermolecular bond energies, the result being

$$c_e = c_0 \exp(-Q/2kT) \tag{3.87}$$

c_0 is a reference concentration and $Q > 0$ given by

$$Q = z\varepsilon + z_0\varepsilon_0 \tag{3.88}$$

is the binding energy of an amphiphile molecule in the bilayer; ε and ε_0 (positive for attraction, negative for repulsion) are, respectively, the energies of the lateral and normal bonds (due to short range surface forces) between the nearest neighbor amphiphile molecules in the bilayer; z and z_0 are the lateral and normal coordination numbers of these molecules (e.g., $z = 6$, $z_0 = 1$ or 3 for hexagonal packing). For steady-state nucleation the nucleation theory derives the explicit $\tau(c_s)$ dependence of the bilayer mean lifetime τ on the bulk concentration c_s

$$\tau(c_s) = \mathrm{A}\exp[\mathrm{B}/\ln(c_e/c_s)] \tag{3.89}$$

with

$$\mathrm{A} = 1/Z\omega N_0 \mathrm{A}$$

and

$$\mathrm{B} = \pi A_0 \tau_L^2/2(kT)^2 \tag{3.90}$$

where Z is the so-called Zeldovich factor (a number from about 0.01 to 1); A is the bilayer area; ω (s^{-1}) is a frequency of a vacancy joining the nucleus hole; N_0 (m^{-2}) is the density of available lattice sites on which a vacancy can be formed.

In some cases τ can be so short that experimental observation of the bilayer after its formation is possible only with a certain probability W depending on the resolution time t_r of the particular

equipment used. In direct visual observation of bilayer rupture, for instance, $t_r \approx 0.5$ s, which is the reaction time of the eye. Since observation of the bilayer is possible only if the bilayer has ruptured during the time $t > t_r$, the nucleation theory yields W as a function of $c_s \leq c_e$:

$$W(c_s) = \exp\{-t_r/\mathbf{A} \exp[\mathbf{B}/\ln(c_e/c_s)]\} \tag{3.91}$$

Equations 3.89 and 3.91 show that both τ and W increase sharply with the bulk surfactant concentration c_s in a relatively narrow range. For this reason, a critical concentration c_c for bilayer rupturing in less than τ_c seconds can be defined by the condition $\tau(c_c) = \tau_c$. From Equation 3.89 we obtain

$$c_c = c_e \exp[-\mathbf{A}/\ln(\tau_c/\mathbf{B})] \tag{3.92}$$

The theoretical $\tau(c_s)$ dependence Equation 3.89 can be easily checked since both τ and c_s are measurable quantities. The bulk concentration c_s of the amphiphile molecules is determined when preparing the surfactant solution and the mean lifetime τ is measured as the time elapsing from the moment of formation of a bilayer with a given radius until the moment of its rupture. Due to the fluctuation character of the film rupture, the film lifetime τ is a random parameter. Experimentally, τ has been determined by averaging from a great number of measurements.

A comparative investigation [104] of the rupture of microscopic emulsion and foam bilayers obtained from the same aqueous solutions of $Do(EO)_{22}$ (dodecyl 22-oxyethyl, a nonionic surfactant) at electrolyte concentration $c > c_{cr}$ has been carried out. The emulsion bilayer was formed between two oil phases of nonane. Figure 3.28 shows the $\tau(c_s)$ dependence for foam (open circles) and emulsion (black circles) bilayer films. In both cases τ depends strongly on the

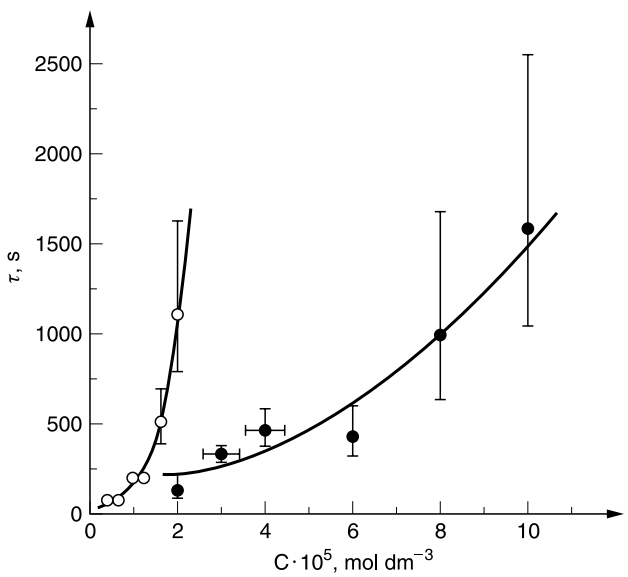

FIGURE 3.28 Mean lifetime τ of Newton black films (bilayer films) vs. surfactant concentration c. Microscopic ($r = 100$ μm) emulsion (●) and foam (○) bilayers from dodecyl 22-oxyethyl + 0.3 M KCl aqueous solutions. (From H.J. Müller, B. Balinov, and D. Exerowa, *Colloid Polymer Sci.* 266: 921 (1988).)

surfactant concentration. The solid curve for the foam bilayer represents the best-fit dependence of Equation 3.89 with A = 0.145 s, B = 25, and $c_e = 3.3 \times 10^{-5}$ mol dm^{-3}. It is seen that the stability of the foam bilayers is greater than that of the emulsion bilayers and that c_e is much higher for the emulsion bilayers.

The same experiment can be also used to check Equation 3.91, W being determined as the ratio between the number of bilayer films observed and number of all films studied. Studying the $W(c_s)$ dependence is possible and particularly convenient at low c_s values when the bilayer mean lifetime τ is comparable with t_r. A characteristic feature of W, according to Equation 3.91, is its sensitivity to changes of c_s in a very narrow range only. The $W(c_s)$ dependence obtained fits well to Equation 3.91 and its shape is different for different types of surfactants [105].

It follows from the theory that $c_c = c_e$ in the case of a missing metastable region when only thermodynamically stable foam bilayers are formed. The high stability of DMPC foam bilayers gives reason to assume that $c_c = c_e$, thus permitting to calculate the binding energy Q from the experimental dependence of c_c on temperature. The values of Q obtained from the best fit of Equation 3.87 to the experimental data are $(1.93 \pm 0.04) \times 10^{-19}$ J at $T < 23\,^{\circ}$C and $(8.03 \pm 0.19) \times 10^{-20}$ J at $T > 23\,^{\circ}$C.

The good agreement between theory and experiment allows the determination of several quantities of the theory: w^*, I^*, τ_L, c_c, c_e, etc. This offers an interesting possibility for the evaluation of some molecular characteristics of the bilayers. For example, from the hole edge energy τ_L the bond energy ε between two nearest-neighbor surfactant molecules in the bilayer plane may be estimated. This important parameter for the bilayer stability and permeability has been determined for various surfactants.

3.7 SIMILARITY BETWEEN EMULSION FILMS AND FOAM FILMS

The comparison of the results for foam films with those for emulsion films, especially the OWO films, is reasonable since in both cases the thin aqueous film is in contact with two hydrophobic phases. It is anticipated that the effects related to adsorption and orientation of surfactant molecules at the film/hydrophobic phase interface are very similar. Hence, some regularities established for aqueous foam films can be applied to OWO emulsion films and vice versa.

Analogous to foam films, stable (or metastable) emulsion films are formed only in the presence of surfactants (emulsifiers) at concentrations higher than the critical concentration of formation of black films c_{bl}. For each emulsifier the latter is a function of temperature, electrolyte content, pH, and presence of other surfactants in the water or organic phase. Unlike the foaming agents c_{bl} of emulsifiers depends also on the nature of the nonpolar ("oil") phase.

The comparison of the concentrations c_{bl} corresponding to formation of black spots in emulsion and foam films, obtained from solutions of one and the same surfactant (which is both emulsifier and foaming agent), indicates that c_{bl} for foam films is considerably lower than c_{bl} for emulsion films. This means that stable foam films (usually black films) can be obtained at lower surfactant concentrations than stable emulsion films even from the nonpolar organic phase. With increasing polarity of the molecules of the organic phase c_{bl} for emulsion aqueous films increases which is analogous to the increase in c_{bl} for hydrocarbon emulsion films. The concentration c_{bl} for emulsion films is close to the emulsifier concentration at which it is possible to disperse a small quantity of the organic phase in a certain volume of the aqueous surfactant solution under definite conditions resulting in formation of stable emulsions.

The process of expansion of a black emulsion film is quite similar to that one in a foam film: at low electrolyte concentrations the black spots in both types of films expand slowly; at high electrolyte concentrations the process is very fast (within a second or less) and ends up with

the formation of a black film with large contact angle film/bulk liquid phase (meniscus). In the process of transformation of the black spots into a black film, the emulsion film is very sensitive to any external effects (vibrations, temperature variations, etc.) in contrast to the black foam film.

As in the case of foam films the thickness of aqueous emulsion films depends on the electrolyte concentration c. Depending on c two types of black films can be formed: CBF and NBF. In contrast to foam films, the OWO emulsion films become NBF at much higher electrolyte concentrations. This peculiarity can be explained with the weaker molecular attraction in emulsion films and the resulting increase in the barrier of the $\Pi(h)$ isotherm. The Hamaker constant A for emulsion films is by a decimal order of magnitude lower than that of aqueous foam films and is within the range between 10^{-21} and 10^{-20} J depending on the surfactant kind and the nature of the organic phase. It should be noted that in the absence of a surfactant, the values of the Hamaker constant of aqueous and nonaqueous emulsion films are equal.

At large surfactant concentrations emulsion films as well as foam films exhibit a layer-by-layer thinning (stratification) and metastable black films are formed. Compared to foam films of analogous composition, the respective emulsion films were thicker, due to the weaker molecular attraction, and the stratification occurred at lower surfactant concentrations. Such a behavior has been reported also for hydrocarbon films (WOW emulsion films).

The dependence of the lifetime of NBF on surfactant concentration of emulsion films stabilized with 22-oxythylated dodecyl alcohol is in conformity with the theory of bilayer stability (see Section 3.6.4). The values of the equilibrium concentrations c_e calculated for emulsion films are higher than those for foam films. It is worth noting that $c_e <$ CMC of foam films from certain surfactants, while for emulsion films $c_e >$ CMC. That is why it is impossible to obtain thermodynamically stable emulsion NBF. This result is of particular importance for the estimation of stability of O/W emulsions. There is a correlation between the stability of single OWO emulsion films, single drops under oil/water interfaces, and real O/W emulsions.

It should be noted as well that the difference between aqueous emulsion films and foam films involves also the dependences of the various parameters of these films (potential of the diffuse double electric layer, surfactant adsorption, surface viscosity, etc.) on the nature of the organic phase, the distribution of the emulsifier between water and organic phase, and the relatively low, as compared to the water/air interface, interfacial tension.

REFERENCES

1. I Newton. Optics. London: Smith & Watford, 1704.
2. I Plateau. Statique Expérimentale et Théorétique des Liquides Soumis aux Seulles Forces Moléculaires. Paris: Dauthier-Villars, 1873.
3. C Marangoni. Nuovo Cimento, Ser 2: 239, 1872.
4. JW Gibbs. Collected Works. London: Longmans Green, 1928.
5. J Perrin. Ann Phys Paris 10: 160, 1918.
6. BV Derjaguin, EV Obukhov, Acta Physicochim USSR 5: 1, 1936.
7. BV Derjaguin, LD Landau. Acta Physicochim USSR 14: 633, 1941.
8. EJW Verwey, JThG Overbeek. Theory of Stability of Lyophobic Colloids. Amsterdam: Elsevier, 1948.
9. JC Eriksson, BV Toshev. Colloids Surfaces 5: 241, 1982.
10. A Scheludko. Annuaire Univ Sofia, Fac Chimie 62: 47, 1970.
11. BV Toshev, IB Ivanov. Colloid Polymer Sci 253: 558, 593, 1975.
12. CJ Vašiček. Optics of Thin Films. Amsterdam: North Holland Publish Co, 1960.
13. A Scheludko, D Platikanov. Kolloid-Z 175: 150, 1961.
14. A Scheludko. Proc Koninkl Nederl Akad Wetenschap B65: 76, 1962.
15. EM Duyvis. PhD Thesis. University of Utrecht, 1962.

16. A Scheludko, D Exerowa. Comm Dept Chem, Bulg Acad Sci 7: 123, 1959.
17. D Exerowa, M Zacharieva, R Cohen, D Platikanov. Colloid Polymer Sci 257: 1089, 1979.
18. D Exerowa, A Scheludko. Compt Rend Acad Bulg Sci 24: 47, 1971.
19. H Sonntag, J Netzel, H Klare. Kolloid-Z Z Polym 211: 121, 1966.
20. PM Kruglaykov, YuG Rovin. Fizikokhimiya chernykh uglevodorodnykh plenok (in Russian). Moscow: Nauka, 1978.
21. D Exerowa, T Kolarov, Khr Khristov. Colloids Surfaces 22: 171, 1987.
22. V Bergeron, CJ Radke. Langmuir 8: 3020, 1992.
23. A Scheludko, B Radoev, T Kolarov. Trans Faraday Soc 64: 2213, 1968.
24. T Kolarov, A Scheludko, D Exerowa. Trans Faraday Soc 64: 2864, 1968.
25. DA Haydon, JT Taylor. Nature 217: 739, 1968.
26. O Reynolds. Phil Trans Royal Soc A177: 157, 1886.
27. JS Stephan. Math Natur Akad Wiss 69: 713, 1884.
28. A Scheludko. Kolloid-Z 155: 39, 1957.
29. J Lyklema, PC Scholten, KJ Mysels. J Phys Chem 69: 116, 1965.
30. V Levich. Physicochemical Hydrodynamics. Engelwood Cliffs: Prentice Hall, 1962.
31. E Mileva, B Radoev. Colloid Polymer Sci 263: 587, 1985; 264: 823, 1986.
32. J Lee, T Hodgson. Chem Eng Sci 23: 1375, 1968.
33. A Scheludko. Adv Colloid Interface Sci 1: 391, 1967.
34. E Mileva, B Radoev. Colloid Polymer Sci 264: 965, 1986.
35. B Radoev, E Manev, I Ivanov. Kolloid-Z 234: 1037, 1969.
36. A Barber, S Hartland. Canad J Chem Eng 54: 279, 1976.
37. E Mileva, B Radoev. Colloids Surfaces A 74: 259, 1993.
38. A Scheludko. Annuaire Univ Sofia, Fac Chim 59: 263, 1964/65.
39. S Frankel, K Mysels. J Phys Chem 66: 190, 1962.
40. D Platikanov. J Phys Chem 68: 3619, 1964.
41. D Exerova, T Kolarov. Annuaire Univ Sofia, Fac Chim 59: 207, 1964/65.
42. O Velev, T Gurkov, R Borwankar. J Colloid Interface Sci 159: 497, 1993.
43. J Joye, G Hirasaki, C Miller. Langmuir 10: 3174, 1994.
44. E Mileva, D Exerowa, in Proceedings of Second World Congress on Emulsion, Bordeaux 2: 2-2-235/1-10, 1997.
45. E. Manev, R Tsekov, B Radoev. J Dispers Sci Technol 18: 769, 1997.
46. B Radoev, A Scheludko, E Manev. J Colloid Interface Sci 95: 254, 1983.
47. E Mileva, B Radoev. Chapter 6 in D Petzev, ed. Emulsions: Structure, Stability and Interactions. Amsterdam: Elsevier–Academic Press, 2004.
48. L Mandelstam. Ann Physik 41: 609, 1913.
49. A Scheludko. Proc Koninkl Nederl Akad Wetenschap B65: 87, 1962.
50. A Vrij. Faraday Discussion Chem Soc 42: 23, 1966.
51. R Tsekov, B Radoev. Adv Colloid Interface Sci 38: 353, 1992.
52. A Sharma, E Ruckenstein. Langmuir 3: 760, 1987.
53. D Exerowa, A Scheludko, in JThG Overbeek, ed. Chemistry, Physics and Application of Surface Active Substances. London: Gordon & Breach, 2: 1097, 1964.
54. JA de Feijter. Chap.1 in I Ivanov, ed. Thin Liquid Films. New York: Marcel Dekker, 1988.
55. BV Deryagin, NV Churaev. Kolloidny Zhur 38: 402, 1976.
56. AI Rusanov. Kolloidny Zhur 28: 583, 1966.
57. BV Toshev, D Platikanov. Adv Colloid Interface Sci 40: 157, 1992.
58. T Kolarov, Z Zorin, D Platikanov. Colloids Surfaces 51: 37, 1990.
59. HM Princen, SG Mason. J Colloid Sci 20: 156, 1965.
60. BV Derjaguin, GA Martynov, YuV Gutop. Kolloidny Zhur 27: 298, 1965.
61. VS Veselovskij, VN Pertsov. Zhur Fiz Khim 8: 245, 1936.
62. BV Derjaguin, NV Churaev, VM Muller. Surface Forces. New York: Consult Bureau, 1987.
63. JN Israelachvili. Intermolecular and Surface Forces, New York: Academic Press, 1991.
64. HBG Casimir, D Polder. Phys Rev 73: 360, 1948.

65. WA Donners. PhD Thesis. University of Utrecht, 1976.
66. A Scheludko, D Exerowa. Kolloid-Z 165: 148, 1959; 168: 24, 1960.
67. J Lyklema, KJ Mysels. J Am Chem Soc 87: 2539, 1965.
68. D Exerowa. Kolloid-Z 232: 703, 1969.
69. D Exerowa, D Kashchiev, D Platikanov. Adv Colloid Polymer Sci 40: 201, 1992.
70. RW Huddelston, AL Smith, in AJ Akers, ed. Foams. New York: Academic Press, 1976.
71. D Exerowa, R Sedev, R Ivanova, T Kolarov, ThF Tadros. Colloids Surfaces 123: 277, 1997.
72. P Flory. Principles of Polymer Chemistry. New York: Cornell University Press, 1956.
73. PG de Gennes. Macromolecules 13: 1069, 1980.
74. J Lyklema, T van Vliet. Faraday Discuss Chem Soc 65: 25, 1978.
75. R Sedev, D Exerowa. Adv Colloid Interface Sci 83: 111, 1999.
76. ES Johnonnott. Phil Mag 11: 746, 1906.
77. HG Bruil, J Lyklema. Nature Phys Sci 233: 19, 1971.
78. A Nikolov, D Wasan. Langmuir 8: 2985, 1992.
79. JW Keuskamp, J Lyklema, in KL Mittal, ed. Adsorption at Interfaces. Washington: ACS Symposium Series 8: 191, 1975.
80. AD Nikolov, PA Kralchevsky, IB Ivanov, DT Wasan. J Colloid Interface Sci 138: 13, 1989.
81. V Bergeron, CJ Radke. Colloid Polymer Sci 273: 165, 1995.
82. L Ter Minassian-Saraga, ed. Thin Films Including Layers: Terminology in Relation to Their Preparation and Characterization. Pure & Appl Chem 66: 1667, 1994.
83. D Exerowa, PM Kruglyakov. Foam and Foam Films. Amsterdam: Elsevier, 1998.
84. J de Feijter, A Vrij. J Colloid Interface Sci 70: 456, 1979.
85. F Huisman, KJ Mysels. J Phys Chem 73: 489, 1969.
86. KJ Mysels, M Jones. Discuss Faraday Soc 42: 42, 1966.
87. IJ Black, RM Herrington. J Chem Soc, Faraday Trans 91: 4251, 1995.
88. T Kolarov, R Cohen, D Exerowa. Colloids Surfaces A 42: 49, 1989; 129–130: 257, 1997.
89. V Bergeron, A Waltermo, P Claesson. Langmuir 12: 1336, 1996.
90. T Yamanaka, M Hayashi, R Matuura. J Colloid Interface Sci 88: 458, 1982.
91. R Cohen, R Koynova, B Tenchov, D Exerowa. Eur Biophys J 20: 203, 1991.
92. R Cohen, D Exerowa, T Yamanaka. Langmuir 12: 5419, 1996.
93. R Cohen, D Exerowa, T Kolarov, T Yamanaka, VM Muller. Colloids Surfaces 65: 201, 1992.
94. T Yamanaka, T Tano, O Kamegaya, D Exerowa, R Cohen. Langmuir 10: 1871, 1994.
95. M Jones, K Mysels, P Scholten. Trans Faraday Soc 62: 1336, 1966.
96. D Platikanov, M Nedyalkov. Annuaire Univ Sofia, Fac Chim 64: 353, 1969/70.
97. D Platikanov, N Rangelova, in BV Deryagin, ed. Research in Surface Forces. New York: Consultants Bureau 4: 246, 1972.
98. D Exerowa, Khr Khristov, M Zacharieva, in Poverkhnostnye sily v tonkikh plenok (in Russian). Moscow: Nauka, 1979.
99. J Corkill, J Goodman, C Orgden, J Tate. Proc Roy Soc A 273: 84, 1963.
100. D den Engelsen, G Frens. J Chem Soc Faraday Trans I 70: 237, 1974.
101. O Belorgey, JJ Benattar. Phys Rev Lett 66: 313, 1991.
102. D Exerowa, D Kashchiev. J Colloid Interface Sci 77: 501, 1980.
103. D Exerowa, D Kashchiev. Contemp Phys 27: 429, 1986.
104. HJ Müller, B Balinov, D Exerowa. Colloid Polymer Sci 266: 921, 1988.
105. D Exerowa, B Balinov, A Nikolova, D Kashchiev. J Colloid Interface Sci 95: 289, 1983.
106. T Kolarov, A. Scheludko, D Exerowa. Annuaire Univ Sofia, Fac Chim 62: 75, 1967/68.